**Atmospheric
Chemistry
and Physics**

Primary sources of $PM_{2.5}$ organic aerosol in an industrial Mediterranean city, Marseille

I. El Haddad[1]**, N. Marchand**[1]**, H. Wortham**[1]**, C. Piot**[2,3]**, J.-L. Besombes**[2]**, J. Cozic**[3]**, C. Chauvel**[4]**, A. Armengaud**[5]**,
D. Robin[5]**, and J.-L. Jaffrezo**[3]

[1]Universités d'Aix-Marseille-CNRS, UMR 6264: Laboratoire Chimie Provence, Equipe Instrumentation et Réactivité Atmosphérique, Marseille, 13331, France
[2]Laboratoire de Chimie Moléculaire et Environnement, Université Savoie-Polytech'Savoie, Chambéry, France
[3]Université Joseph Fourier-Grenoble 1-CNRS, UMR 5183, Laboratoire de Glaciologie et Géophysique de l'Environnement, Saint Martin d'Hères, 38402, France
[4]Université Joseph Fourier-Grenoble 1-CNRS, UMR 5025, Laboratoire de Geodynamique des Chaines Alpines, BP 53, Grenoble, 38048, France
[5]Regional Network for Air Quality Monitoring (ATMO-PACA), 146 rue Paradis 13006 Marseille, France

Abstract. Marseille, the most important port of the Mediterranean Sea, represents a challenging case study for source apportionment exercises, combining an active photochemistry and multiple emission sources, including fugitive emissions from industrial sources and shipping. This paper presents a Chemical Mass Balance (CMB) approach based on organic markers and metals to apportion the primary sources of organic aerosol in Marseille, with a special focus on industrial emissions. Overall, the CMB model accounts for the major primary anthropogenic sources including motor vehicles, biomass burning and the aggregate emissions from three industrial processes (heavy fuel oil combustion/shipping, coke production and steel manufacturing) as well as some primary biogenic emissions. This source apportionment exercise is well corroborated by ^{14}C measurements. Primary OC estimated by the CMB accounts on average for 22% of total OC and is dominated by the vehicular emissions that contribute on average for 17% of OC mass concentration (vehicular PM contributes for 17% of $PM_{2.5}$). Even though industrial emissions contribute only 2.3% of the total OC (7% of $PM_{2.5}$), they are associated with ultrafine particles ($Dp < 80$ nm) and high concentrations of Polycyclic Aromatic Hydrocarbons (PAH) and heavy metals such as Pb, Ni and V. On one hand, given that industrial emissions governed key primary markers, their omission

would lead to substantial uncertainties in the CMB analysis performed in areas heavily impacted by such sources, hindering accurate estimation of non-industrial primary sources and secondary sources. On the other hand, being associated with bursts of submicron particles and carcinogenic and mutagenic components such as PAH, these emissions are most likely related with acute ill-health outcomes and should be regulated despite their small contributions to OC. Another important result is the fact that 78% of OC mass cannot be attributed to the major primary sources and, thus, remains un-apportioned. We have consequently critically investigated the uncertainties underlying our CMB apportionments. While we have provided some evidence for photochemical decay of hopanes, this decay does not appear to significantly alter the CMB estimates of the total primary OC. Sampling artifacts and unaccounted primary sources also appear to marginally influence the amount of un-apportioned OC. Therefore, this significant amount of un-apportioned OC is mostly attributed to secondary organic carbon that appears to be the major component of OC during the whole period of study.

1 Introduction

Tougher particulate matter (PM) regulations around the world and especially in Europe point out the need of source apportionment studies in order to better understand the

different sources of aerosol and quantify their contributions to atmospheric load. Organic aerosol (OA) is a major component of fine particulate matter accounting on average for half of the total PM$_{2.5}$ dry mass, and it remains the less understood fraction of the aerosol (Jimenez et al., 2009; Kanakidou et al., 2005; Putaud et al., 2004). OA is a highly complex mixture in constant evolution, emitted from several primary sources including anthropogenic sources (vehicular emissions, wood burning, industrial processes, cooking operations. . .) and natural sources (vegetative detritus. . .). OA is also formed in situ in the atmosphere from the oxidation of gas-phase precursors and subsequent partitioning of the less volatile products into the particle phase (secondary organic aerosol-SOA). Although recent studies have targeted a number of approaches to identify and quantify both primary and secondary sources, none of these techniques can be considered as absolute, each of them presenting shortcomings and uncertainties.

One of the most widely used approaches to investigate PM sources is the Chemical Mass Balance (CMB) used in conjunction with organic molecular markers and/or metals (see, for example, Schauer and Cass, 2000; Schauer et al., 1996, 2002a; Watson et al., 1998). This technique draws upon highly specific chemical source markers (e.g., hopanes, levoglucosan. . .) to estimate the contribution of emissions from major primary sources. The technique cannot quantify secondary sources, but the residual organic carbon not attributed to any primary sources in the model is commonly considered as secondary organic carbon (SOC). CMB modelling has been applied to various types of atmospheres and the results highlight a strong seasonal variation. In wintertime, these results suggest a dominant contribution of primary sources (Favez et al., 2010; Schauer and Cass, 2000; Sheesley et al., 2007). Conversely, during summer, the main part of the ambient OC cannot be apportioned to primary sources (Schauer et al., 2002a; Zheng et al., 2006), which is qualitatively consistent with the characteristics of SOA formation. Thus, it is particularly interesting to apply the CMB approach in Mediterranean environments, known for their intense photochemistry (Flaounas et al., 2009).

CMB modelling suffers from a number of uncertainties that are not explicitly considered by the model, but can greatly influence source increments (Robinson et al., 2006a, b, c, d; Subramanian et al., 2007). First, CMB relies heavily on the selection of source profiles, all the more since footprints of a number of sources such as industrial emissions remain poorly characterised. Further, photochemical decay of the chemical markers and evaporation of both chemical markers and OC during atmospheric transport from source points to the receptor site can bias the estimates of source contributions. Finally, unknown primary sources of markers or of OC can also influence the source apportionment results. As a consequence, CMB modelling analyses are regularly constrained by complementary source apportionment techniques, mainly radiocarbon (^{14}C) analysis and Positive Ma-

trix Factorisation associated with Aerosol Mass Spectrometer data (AMS/PMF) (Docherty et al., 2008; Favez et al., 2010; Zheng et al., 2006).

This paper is the first paper of a two-part series investigating the sources of organic aerosol during summertime in Marseille, a major French Mediterranean city. Results were obtained as part of the FORMES project during a 15-day intensive field campaign held in Marseille during summer 2008. These two papers capitalize on off-line measurements including determination of organic molecular markers, metals, ^{14}C, WSOC (water soluble organic carbon), OC/EC and major ions. This dataset offers the opportunity for a global insight into the organic aerosol characteristics and main sources, and enables to critically evaluate CMB results in comparison with other approaches. This paper is devoted to source apportionment of primary sources of organic aerosol with a special emphasis on CMB modelling of industrial emissions which have been rarely investigated in previous CMB studies. Because CMB approach is highly sensitive to source profiles and to the included markers, we adopt a multistep approach in order to determine the main influencing primary sources and accurately assess their contributions. This approach involves a preliminary principal component analysis (PCA) and a careful investigation of marker trends, ratios and source profiles. Impacts of CMB modelling common biases and uncertainties on the results are also critically discussed. The second paper entitled "Insights into the secondary fraction of the organic aerosol in a Mediterranean urban area: Marseille" explores the secondary fraction of OA.

2 Methods

2.1 Site description and sample collection

The intensive field campaign was conducted during summer 2008, from 30 June to 14 July, at an urban background site located in the downtown park "Cinq Avenues" (43°18′20″ N, 5°23′40″ E, 64 m a.s.l.) in Marseille (Fig. 1). Marseille is the second most populated city in France with more than 1 million inhabitants. With traffic of about 97 million tons (Mt) (62.5% of which are crude oil and oil products) in 2007, Marseille is also the most important port of the Mediterranean Sea. It handles twice the traffic compared to Genoa and nearly three times the traffic of Barcelona or Valencia. Marseille is also in the vicinity of the large petrochemical and industrial area of Fos-Berre, located 40 km northwest of the metropolitan area (Fig. 1). The main industries include petroleum refining, shipbuilding, steel facilities and coke production. This area is also well known for its photochemical pollution, especially regarding ozone (Flaounas et al., 2009), and evidences of rapid formation of secondary organic aerosol have been pointed out within the frameworks of the ESCOMPTE experiment (Cachier et al., 2005; Drobinski et al., 2007) and the BOND project (Petäjä et al., 2007).

Air masses circulation in the area of Marseille is complex (Drobinski et al., 2007; Flaounas et al., 2009). However, two particular situations occur frequently during summertime: the Mistral and sea breeze conditions (Fig. 1). Mistral is a strong regional wind that blows down from the north along the lower Rhône River valley toward the Mediterranean Sea. In low Mistral ($<3\,\mathrm{m\,s^{-1}}$) conditions, sea breeze circulation prevails and is often associated with high pollution levels over Marseille due to the low dispersion of pollutants (Flaounas et al., 2009). In the early morning of such days, Marseille is directly downwind of the industrial area and, as the temperature of the surface of the land rises, sea breeze wind speed increases. It results in an increased residence time of the industrial polluted air masses over the Mediterranean Sea before they arrive over Marseille. Such conditions are characterised by high ozone concentrations associated most of the time with high concentrations of industrial tracers (SO$_2$, metals, and/or PAH). These specific conditions occurred 3 days during our field campaign (i.e., on 30 June, 5 July, and 10 July).

PM$_{2.5}$ were collected continuously on a 12h-basis (05:30 to 17:30 UT, and 17:30 to 05:30 UT, total number of 30 samples) using high volume samplers (Digitel DA80) operating at a flow rate of $30\,\mathrm{m^3\,h^{-1}}$. Particles were collected onto 150 mm-diameter quartz fibre filters (Whatman QMA), preheated at $500\,^\circ\mathrm{C}$ during 3 h. Samples were stored at $-18\,^\circ\mathrm{C}$ in aluminium foil, sealed in polyethylene bags until analysis. Six field blank samples were also prepared following the same procedure.

The submicron aerosol number size distribution in the range 11.1–1083 nm was further investigated using a Scanning Mobility Particle Sizer system (SMPS, L-DMA, CPC5403, GRIMM). Finally, ancillary data including O$_3$, SO$_2$, NO$_x$, PM$_{10}$ and PM$_{2.5}$ mass concentrations were also measured with the standard equipment of the Air Quality Monitoring Network, including a Tapered Element Oscillating Microbalance equipped with a Filter Dynamic Measurement System (TEOM-FDMS, Thermo Scientific) for PM$_{10}$ and PM$_{2.5}$.

2.2 Offline analysis

2.2.1 OC, EC, WSOC and major ions analysis

EC and OC measurements were performed on 1.5 cm^2 of each filter using a Thermo-Optical Transmission (TOT) method on a Sunset Lab analyser (Jaffrezo et al., 2005; Birch and Cary, 1996) following the NIOSH temperature programme (Schmid et al., 2001). Sample fractions of 11.34 cm^2 from HiVol filters are extracted into 15 mL of ultrapure water by 30 min short vortex agitation, in order to analyse major ionic species and water-soluble organic carbon (WSOC). Just before the analysis, samples are filtered using Acrodisc filters (Pall, Gelmann) with a porosity of $0.2\,\mu\mathrm{m}$, previously rinsed with 40 mL of ultrapure water. Sample
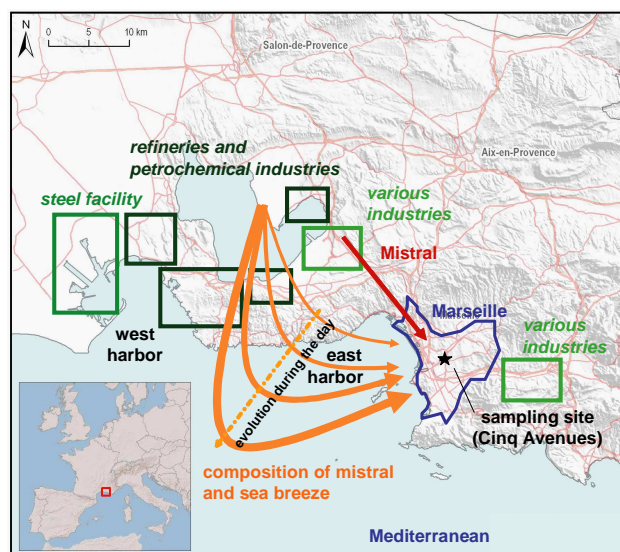

Fig. 1. Location of the sampling site (Cinq avenues) and major nearby industrial facilities and simplified illustration of the main wind circulations (Mistral and land and sea breeze).

analyses of major ionic species are performed using ion chromatography, as described in Jaffrezo et al. (1998). Analysis of cations (Na$^+$, NH$_4^+$, K$^+$, Mg^{2+}) takes place with a CS12 column on a Dionex 100 IC, whereas analysis of anions (Cl$^-$, NO$_3^-$, SO$_4^{2-}$) takes place with an AS11 column on a Dionex 500 IC. The WSOC is quantified with an OI Analytical 700 TOC analyser using persulphate oxidation at $100\,^\circ\mathrm{C}$ of the organic matter, followed by CO$_2$ quantification with a non-dispersive infrared spectrophotometer (Jaffrezo et al., 1998).

Blank levels for each chemical species are calculated from the analysis of procedural blanks and are subtracted from the measured sample concentrations to obtain the actual concentrations. Atmospheric detection limits are calculated as the blank value plus twice the standard deviation of the blank sample concentrations, using a typical sampling duration of 12 h.

2.2.2 Trace elements determination

Fifty chemical elements were measured by ICP-MS following complete dissolution of an aliquot of 11.34 cm^2 taken from the quartz fibre filters. The material is dissolved using a mixture of high-purity concentrated HF and HNO$_3$. After evaporation of the liquid, samples are spiked with a solution containing five pure elements (Be, Ge, In, Tm and Bi) and diluted in 2 mL of 2% HNO$_3$ with traces of HF to be analysed on an Agilent 7500ce ICP-MS. The general procedure follows the technique described by Chauvel et al. (2010), however, some minor modifications are introduced to measure elements not usually analysed. A flow of He is introduced in the collision cell of the ICP-MS to minimize molecular interferences on iron and the same collision cell was filled with

He to measure arsenic as well as all elements with masses ranging from 23 (Na) to 78 (Se). All data are corrected for drift during analyses and the average values measured on the blank filters are subtracted. Concentrations are calculated using the rock reference material BR (Chauvel et al., 2010).

2.2.3 Analysis of organic compounds

Organic compounds were quantified by gas chromatography coupled with mass spectrometry (GC-MS), following the method detailed in El Haddad et al. (2009) and Favez et al. (2010). Prior to extraction, filters are spiked with known amounts of isotope-labelled standards: tetracosane-d50 and cholesterol-d6. Filters are subsequently extracted during 5 min with a dichloromethane/acetone mix (1/1 v:v) using an accelerated pressurized solvent extraction device (ASE 300, Dionex) at 100 °C and 100 bar. The solvent extracts are reduced to a volume of 500 µL using a Turbo Vap II concentrator. The remaining volumes are split into two fractions. The first fraction is directly injected while the second fraction is subjected to derivation for 2 h at 70 °C before GC-MS analysis, using N,O-Bis(trimethylsilyl)-trifluoroacetamide containing 10% trimethyl-chlorosilane. The two fractions are analysed using the same GC-MS conditions detailed in El Haddad et al. (2009), i.e., electron impact ionisation at 70 eV and chromatographic separation on a TR-5MS capillary column (ThermoElectron). GC-MS response factors are determined using authentic standards (Table 1). Compounds for which no authentic standards are available are quantified using the response factor of compounds with analogous chemical structures (Table 1). Field blank filters are also treated following the same procedure.

2.2.4 ^{14}C analysis on total carbon (TC)

Radiocarbon measurements were conducted on HiVol quartz filter fractions ($\sim$40 cm^2) using ARTEMIS Accelerator Mass Spectrometry, at Saclay (CNRS-CEA-IRD-IRSN, France). Each sample is first packed into a pre-fired quartz tube containing CuO and Ag powder. The tube is combusted at 850 °C in a muffle furnace for 4 h. Carbon dioxide (CO$_2$) is collected and purified before its conversion into graphite by hydrogen reduction at 600 °C using Fe catalyst. The modern fraction ($f_{\mathrm{m}} = (^{14}C/^{12}C)_{\mathrm{sample}}/(^{14}C/^{12}C)_{1950}$) is determined as the ratio of $^{14}C/^{12}C$ in aerosol sample to $^{14}C/^{12}C$ in the NBS Oxalic Acid standard (NIST-SRM-4990B) (Stuiver and Polach, 1977).

2.3 CMB model

A Chemical Mass Balance (CMB) model was used in order to apportion the sources of OA. CMB modelling estimates contributions of specific primary sources by solving a system of linear equations in which the concentration of specific chemical constituents in a given ambient sample is described

as arising from a linear combination of the relative chemical compositions of the contributing sources (Watson et al., 1998). Source-specific individual organic compounds of primary origin are most often used in conjunction with the CMB model to apportion sources of primary OC. In this approach, the concentration of selected chemical marker i at receptor site k, C_{ik}, can be expressed as the following linear equation:

$$C_{ik} = \sum_{j=1}^{m} f_{ijk} a_{ij} s_{jk} \tag{1}$$

where m is the total number of emission sources, a_{ij} is the relative concentration of chemical species i in fine OC emitted from source j, s_{jk} is the increment to total OC concentration at receptor site k originating from source j and f_{ijk} is the coefficient of fractionation that represents the modification of a_{ij} during transport from source j to receptor k. The fractionation coefficient accounts for selective loss of constituent i due to atmospheric processes such as chemical aging or gas-particle partitioning related to the dilution of the emissions. Atmospheric oxidation and dilution are nonlinear phenomena, depending on numerous conditions including transport time, ambient temperature, oxidant concentration, etc., and can change drastically the fractionation coefficients (f_{ijk}) of the selected markers as it was observed in the case of hopanes (Sect. 4.4.1). These processes represent a very substantial complication to linear source apportionment techniques such as Chemical Mass Balance and the determination of the f_{ijk} coefficient is highly complicated (Donahue et al., 2006; Robinson et al., 2006a, b, c, d, 2007). Accordingly, CMB modelling uses, as fitting species, key markers that are assumed to be non-volatile and reasonably stable in the atmosphere, implying fractionation coefficients near unity for such species. In order to solve the set of linear equations generated by Eq. (1), an effective variance weighted least squares solution is used. The CMB source allocation was computed using United States Environmental Protection agency EPA-CMB8.2 software.

A critical issue generally encountered in CMB modelling is the selection of the source profiles. This selection relies heavily on two implicit assumptions. First, the aggregate emissions from a given source class are well represented by an average source profile with known marker-to-OC ratios (a_{ij}) and that reflects the most the emission sources influencing the receptor site. Second, all the major sources of the marker compounds have to be included in the model. The selection of the source profiles for non-industrial emissions in France and the sensitivity of the CMB model results with respect to the selected profiles are detailed in Favez et al. (2010). All calculations include vehicular emissions derived from a tunnel study held in Marseille (El Haddad et al., 2009), biomass burning emissions (Fine et al., 2002), vegetative detritus (Rogge et al., 1993a) and natural gas combustion (Rogge et al., 1993b). As discussed in Sect. 3.2.2., three industrial-emission-related profiles were

Table 1. Organic and elemental carbon (µg m^{-3}), main elements (ng m^{-3}) and organic marker concentrations (ng m^{-3}) in PM$_{2.5}$ (average (min-max)).

carbonaceous matter (µg m^{-3})			
OC	4.7 (2.9–9.6)	EC	1.3 (0.66–3.4)
main elements (ng m^{-3})			
Al*	34.7 (8.47–115)	Cu* [225]***	3.29 (0.50–7.27)
V** [262]***	7.18 (0.77–22.7)	Zn* [330]***	10.6 (0.84–45.7)
Mn* [5.26]***	1.41 (0.27–5.14)	Mo* [1600]***	1.63 (0.11–9.08)
Fe* [3.42]***	52.8 (14.6–131)	Pb** [350]***	2.40 (0.57–8.85)
Ni** [1500]***	5.08 (1.85–13.3)		
n-alkanes (ng m^{-3})			
n-pentacosane*,a	2.99 (1.72–4.62)	n-nonacosane (A29)**,b	4.44 (1.48–10.1)
n-hexacosane*,b	1.15 (0.508–2.08)	n-triacontane (A30)**,a	0.901 (0.270–1.63)
n-heptacosane (A27)**,b	2.96 (1.08–5.94)	n-hentriacontane (A31)**,a	3.79 (1.35–7.93)
n-octacosane (A28)**,a	1.19 (0.48–2.07)	n-dotriacontane (A32)*,a	0.712 (0.128–1.32)
polycyclic aromatic hydrocarbons (ng m^{-3})			
benzo[b,k]fluoranthene (BF)**,a	0.337 (0.050–1.69)	indeno[1,2,3-cd]fluoranthene*,c	0.056 (<dl–0.206)
benzo[j]fluoranthene*,a	0.030 (<dl – 0.213)	indeno[1,2,3-cd]pyrene (IP)**,a	0.167 (0.021–0.842)
benzo[e]pyrene (BeP)**,a	0.181 (0.024–0.806)	dibenzoanthracene*,a	0.079 (<dl–0.506)
benzo[a]pyrene*,a	0.142 (0.015–0.855)	benzo-ghi-perylene (BP)**,a	0.177 (0.018–0.659)
Hopanes (ng m^{-3})			
trisnorneohopane*,d	0.038 (0.012–0.078)	17α(H)-21β(H)-hopane (H2)**,a	0.202 (0.091–0.554)
17α(H)-trisnorhopane*,d	0.044 (0.011–0.102)	17α(H)-21β(H)-22S-homohopane (H3)**,d	0.124 (0.049–0.260)
17α(H)-21β(H)-norhopane (H1)**,d	0.231 (0.116–0.609)	17α(H)-21β(H)-22R-homohopane*,d	0.087 (0.028–0.179)
Phthalates esters (ng m^{-3})			
di-isobutyl phthalate*,e	24.2 (6.79–69.4)	di-butyl phthalate*,a	12.2 (2.80–30.3)
benzyl butyl phthalate*,a	0.716 (0.107–3.84)	bis(2-ethylhexyl) phthalate *,a	10.8 (1.79–25.6)
Sugars and sugar derivates (ng m^{-3})			
glucose*,a	4.78 (<dl–27.5)	fructose*,a	0.57 (<dl–2.71)
arabitol*,a	0.51 (<dl–2.40)	mannitol*,a	0.45 (<dl–2.39)
sucrose*,a	0.98 (<dl–7.91)	trehalose*,a	0.11 (<dl–0.57)
levoglucosan (Lev)**,a	5.02 (0.26–18.7)		

dl: detection limit: for PAH dl = 0.012 ng m^{-3}; for sugars dl = 0.05 ng m^{-3};

(* and **) notes: (*) compounds not included in the CMB modelling, (**) compounds included in the CMB modelling.

(a–d) identification and quantification notes: the quantification of the organic compounds is based on the response factors of a – authentic standards, b – average of alkanes with the closer carbon number, c – Indeno[1,2,3-cd]pyrene, d – 17α(H)-21β(H)-hopane, e – Di-butyl phthalate.

*** [EF]: enrichment factor for the elements in the aerosol calculated in comparison with the elemental composition of the upper continental crust (UCC). EF near unity indicates that the element is preliminary derived from crustal dust dust. EF significantly higher than 10 suggests that the abundance of the element in the aerosol is rather controlled by input from anthropogenic sources.

selected: metallurgical coke production (Weitkamp et al., 2005), HFO combustion/shipping (Agrawal et al., 2008) and steel manufacturing (Tsai et al., 2007).

In order to assess contributions from the aforementioned sources, we have used in this particular model as fitting species: levoglucosan as a specific marker for biomass burning, elemental carbon (EC) and three hopanes (i.e., 17α(H),21β(H)-norhopane, 17α(H),21β(H)-hopane and 22S,17α(H), 21β(H)-homohopane) as key mark-

ers for vehicular emissions (Table 1). In addition, a series of C27-C32 n-alkanes were selected since this range demonstrates high odd-carbon preference that is specific to biogenic sources. In order to apportion industrial emissions, Four PAH (benzo[b,k]fluoranthene, benzo[e]pyrene, indeno[1,2,3-cd]pyrene, and benzo[ghi]perylene), V, Ni and Pb (Table 1) were included as fitting species in the CMB, as discussed in Sect. 3.2.1.

3 CMB setup

3.1 Preliminary PCA

A principal component analysis (PCA) is performed as a preliminary approach that allows underscoring the variable main trends and their hierarchical distribution, enabling the identification of the main sources or processes influencing the aerosol components, prior to the CMB analysis. The PCA was performed on 27 active variables comprising concentrations (ng m^{-3}) of 23 different primary emission markers including a series of C27-C32 alkanes, 4 hopanes (17α(H)-trisnorhopane, 17α(H),21β(H)-norhopane (H1), 17α(H),21β(H)-hopane (H2) and 22S,17α(H),21β(H)-homohopane (H3)), 4 high molecular weight polycyclic aromatic hydrocarbons (PAH: benzo[b,k]fluoranthene (BF), benzo[e]pyrene (BeP), indeno[1,2,3-cd]pyrene (IP) and benzo[ghi]perylene (BP)), a set of 8 trace metals (V, Mn, Fe, Ni, Cu, Zn, Mo and Pb) and EC (μg m^{-3}), as well as OC (μg m^{-3}), NH$_4^+$ (μg m^{-3}), NO$_3^-$ (μg m^{-3}) and SO$_4^{2-}$ (μg m^{-3}).

The projection of these variables on the correlation diagram is represented in Fig. 2. The first and second axes, corresponding to F1 and F2 factors, account for 50.6% and 16.2% of the explained variance, respectively. Four clusters are observed. The first cluster (C1) comprises the major ions mostly of secondary origins showing a positive correlation with the first factor (F1). OC also shows a positive correlation with the first factor (F1) suggesting that a significant fraction of the organic aerosol is most probably of secondary origin. The other three clusters (C2, C3, and C4) present a negative correlation with the first factor and are all built on markers of primary emissions. Cluster C2 includes n-alkanes with odd-carbon numbers, which are generally associated with abrasion products from leaf surfaces (Rogge et al., 1993a). Cluster C3 includes n-alkanes with even-carbon numbers, the 4 hopanes and EC, which are markers of vehicular emissions (El Haddad et al., 2009; Schauer et al., 1999, 2002b). The last cluster (C4) gathers all the trace elements and the 4 PAH. Considering the environment of Marseille, this cluster is highly suspected to characterise inputs from industrial emissions.

From this preliminary PCA analysis, the assessment of the 3 primary sources represented by cluster C2, C3 and C4 appears to be of primary importance. If apportionment of non-industrial emissions using CMB is now relatively well constrained, great uncertainties are still associated with the assessment of industrial emissions which could impact heavily CMB results in environments such Marseille.

3.2 Focus on industrial emissions: how to select source profiles and specific markers?

Two major obstacles can be encountered when dealing with the estimation of industrial emissions using CMB modelling: (i) first, primary organic markers emitted from industrial
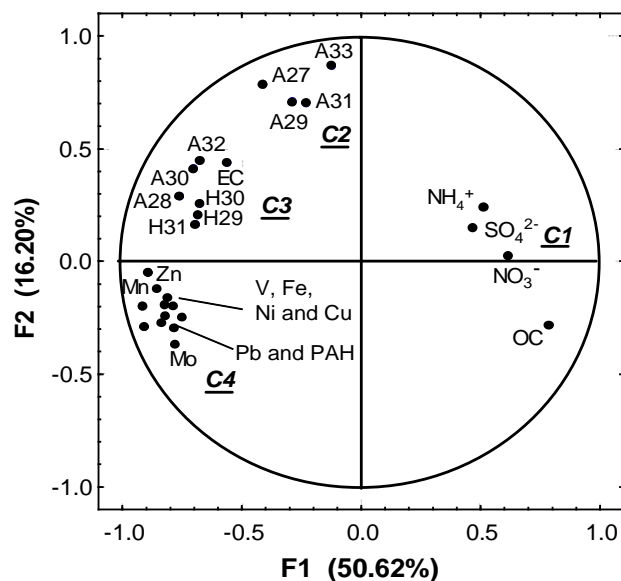

Fig. 2. Principal component analysis projections of 27 variables consisting of concentrations (ng m^{-3}) of 23 different markers including: a series of C27-C32 alkanes (A27-A32), 3 hopanes (17α(H),21β(H)-norhopane (H1), 17α(H),21β(H)-hopane (H2) and 22S,17α(H),21β(H)-homohopane (H4)), 4 PAH (benzo[b,k]fluoranthene, benzo[e]pyrene, indeno[1,2,3-cd]pyrene and benzo[ghi]perylene), a set of 8 elements (V, Mn, Fe, Ni, Cu, Zn, Mo and Pb), and EC, as well as OC and the 3 major ions (NH$_4^+$, NO$_3^-$, SO$_4^{2-}$). F1 and F2 denote the first and the second principal components, respectively. C1, C2, C3 and C4 are the 4 clusters obtained by the PCA.

sources remain among the least constrained, (ii) and second data at emission points are scarce (Agrawal et al., 2008; Rogge et al., 1997a; Tsai et al., 2007; Weitkamp et al., 2005), all the more since there are a great number of industrial processes whose variability can greatly affect the marker source profiles. As a result, comparing the available profiles reveals some very large variations in the marker relative abundances (a_{ij}) that can typically span more than two orders of magnitude, leading to similar variability in the model outputs. Such variability makes the selection of an industrial source profile representative of given industrial emission a major challenge. Such obstacles render the apportionment of these kinds of emissions a challenging issue.

3.2.1 Evidence of the impact of industrial emissions and main markers

Industrial emissions are commonly investigated through the analysis of aerosol elemental composition (Viana et al., 2008, and reference therein). However, metals can also originate from various sources such as mineral dust, vehicular emissions or brake dust, for example (Chow et al., 2003, 2007; Schauer et al., 2006; Thorpe and Harrison, 2008). In order to

clearly reveal the influence of industrial emissions on these elements both Enrichment Factors and temporal trends have to be studied.

Enrichment Factors, EFs, relative to upper continental crust (UCC) for the main elements revealed as potential markers of industrial emissions by the preliminary PCA are reported in Table 1. EFs are computed by normalizing the concentration of each element to Aluminum (Al), an index for mineral dust, and dividing the result by the relative abundance of the same element over Al in UCC (Taylor and McLennan, 1985). EFs close to unity imply that the considered element is primarily derived from crustal dust. In contrast, EFs greater than 10 suggest that the abundance of the considered element in the aerosol is rather controlled by inputs from anthropogenic sources. V, Ni, Cu, Zn, Mo and Pb show high EFs ranging between 225 and 1600, highlighting their anthropogenic origins, whereas Fe and Mn present EFs smaller than 10, suggesting that mineral dust represents a predominant source for these elements (Table 1).

Time series of V, Ni, and Pb (Fig. 3a) show that the concentrations of these elements follow during the campaign remarkable variations characterised by several episodes with ten-fold enhancements. The analyses of air masses backward trajectories, MM5 wind fields and local wind observation straightforwardly relate the observed spikes to regional transport of air masses from the industrial area of Fos-Berre. A typical example is presented in Fig. 3b. This provides clear evidence that industrial emissions drives the concentrations of these trace metals in the Marseille area. Several studies indicate that V and Ni are typical products of heavy fuel oil (HFO) combustion in industrial boilers or ship engines (Agrawal et al., 2008; Ntziachristos et al., 2007; Suarez and Ondov, 2002; Viana et al., 2008). Meanwhile, Pb sources in urban are less constrained and recent measurements point towards a global increase of Pb concentrations even after the ban on leaded petrol, suggesting that nonautomotive-related sources of this element are becoming important worldwide (Osterberg et al., 2008). High concentrations and enrichment factors of Pb were often reported in urban environments in the vicinity of industrial areas (Pina et al., 2002; Querol et al., 2007; Viana et al., 2008), which is consistent with the high emission factors of this element in aerosol derived from metal smelting (Tsai et al., 2007). During the sampling period, the other anthropogenic-dominated heavy metals (Zn, Cu and Mo) that can be also emitted during metal manufacturing follow trends similar to that of V, Ni, and Pb. Furthermore, it is worth mentioning that Fe and Mn levels, together with their enrichment factors, also experience to some extent the increase during the episodes ascribed to industrial emissions, suggesting some anthropogenic emissions for these species.

Among the heavy metals of anthropogenic origins, Cu, Zn and Mo cannot be included in the CMB modelling since other primary non-industrial sources (e.g., brake lining, lube-oil combustion and tyre wear) that are not considered here may
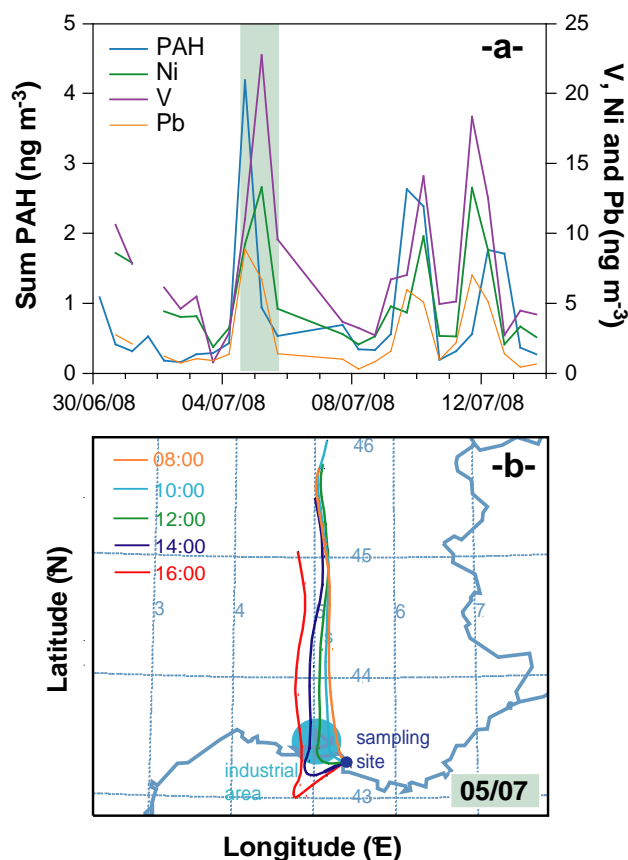

Fig. 3. (a) Time series of the industrial emission markers: V, Ni, Pb and sum of heavy PAH (benzo[b,k]fluoranthene, benzo[e]pyrene, Indeno[1,2,3-cd]pyrene and Benzo-ghi-perylene). (b) HYSPLIT air mass backward trajectory (Rolph, 2010) illustrating the overall air masses circulation occurring during a typical industrial events (5 July 2008 08:00–16:00). Backward trajectories are confirmed by both MM5 modelling and local winds measurements.

contribute significantly to their concentrations in urban locations (Schauer et al., 2006; Thorpe and Harrison, 2008). While the presence of V, Ni and Pb cannot be excluded in traffic related emissions, dynamometer chassis experiments (Schauer et al., 1999, 2002b; Schauer et al., 2006) and tunnel studies (Geller et al., 2005; Grieshop et al., 2006) converge to the same conclusion that these elements are present only in trace amounts, with concentrations lower by one to two orders of magnitude compared to the amounts measured when the site was directly downwind of industrial area. Consequently, it can be considered that V, Ni and Pb are mainly resulting from industrial and shipping emissions in our case, and they can be included in the CMB model as quasi-exclusive markers of these emissions.

High molecular weight PAH (benzo[b,k]fluoranthene, benzo[e]pyrene, indeno[1,2,3-cd]pyrene and benzo[ghi]perylene), commonly used as molecular markers in CMB modelling, are emitted by numerous combustion

sources, including motor vehicles (mainly gasoline vehicles), biomass burning and industrial processes (Robinson et al., 2006d). In our case, the temporal variation of the sum of high molecular weight PAH displays a pattern similar to that of heavy metals (Fig. 3), implying an overwhelming contribution of the industrial processes to PAH concentrations in Marseille. In addition, a preliminary CMB analysis performed without taking into consideration any industrial source indicates that the other major combustion sources included in the model (vehicular emissions and biomass burning) account for less than 5% of the heavy PAH observed in Marseille. This test supports the fact that there are unaccounted sources of PAH (hence, of primary OC) that have to be taken into consideration in the CMB model and the omission of such sources would lead to substantial uncertainties in the estimation of non-industrial primary sources and secondary sources by the CMB. Amongst these influencing industrial sources, coke production, coke combustion and fuel combustion can generate PM emissions particularly rich in heavy molecular weight PAH (Agrawal et al., 2008; Weitkamp et al., 2005; Zhang et al., 2008). Consequently, PAH (benzo[b,k]fluoranthene, benzo[e]pyrene, indeno[1,2,3-cd]pyrene and benzo[ghi]perylene) can be used as effective markers of these emissions.

3.2.2 Source profiles for industrial emissions

The above results brought clear evidence that industrial emissions can potentially represent an important source of aerosol and some key markers for these emissions were identified. However, in order to select chemical profiles representative of industrial emissions, we have cautiously analysed the ambient ratios between the identified industrial markers and compared them to emission ratios from the literature. Regarding the Marseille area, the major industrial processes are: HFO combustion/shipping (Agrawal et al., 2008), coke production (Weitkamp et al., 2005) and steel manufacturing (Tsai et al., 2007). Ambient ratios between the industrial markers (PAH, V, Ni and Pb) are presented as a box-and-whisker diagram in Fig. 4. The spacing between the different parts of a box indicates the degree of dispersion in the ambient ratios and non-disperse ratios point to the predominance of a single source of markers with a constant profile.

Figure 4 shows that ambient ratios between the different PAH (IP-to-BeP and BP-to-BeP) are highly stable, which is not unexpected since these PAH displayed a constant profile during the sampling period. Furthermore, these ratios are consistent with the emission ratios of coke production (Weitkamp et al., 2005), a major source of PAH in industrial areas (Robinson et al., 2006d). It is worthwhile to note that the industrial area of Fos Berre includes one of the largest metallurgical coke production facilities in France. Likewise, Ni and V also show constant ambient ratios (1.3 ± 0.2), slightly lower than the characteristic ratio for HFO combustion within ship engines (2.3 ± 0.5) (Agrawal et al., 2008).
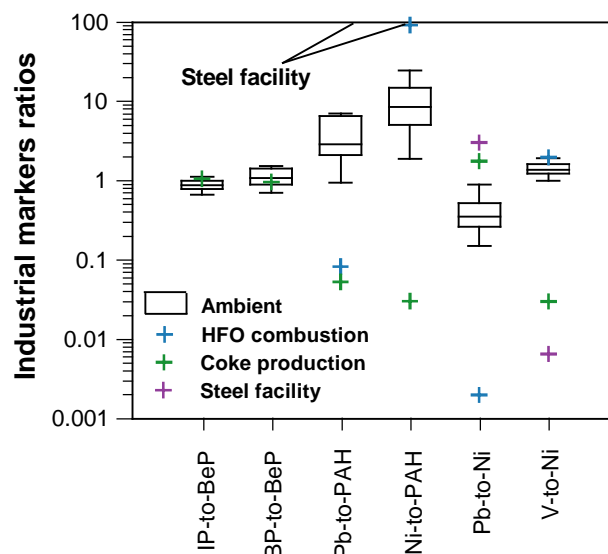

Fig. 4. Ambient ratios between industrial markers (PAH, V, Ni and Pb) represented as box-and-whisker diagram. The bottom and top of the box denote the lower and upper quartiles, respectively (the 25th and 75th percentile), and the band inside the box is the median (the 50th percentile). The ends of the whiskers refer to the 8th percentile and the 92nd percentile. For comparison, emission ratios are also shown for different industrial sources: HFO combustion/shipping (Agrawal et al., 2008; Rogge et al., 1997b), coke production (Weitkamp et al., 2005) and steel facility (Tsai et al., 2007). The spacing between the different parts of the box indicates the degree of dispersion and skewness in the data. Non-dispersed ratios point to the predominance of a single source of markers.

In contrast, widely varying ambient ratios between PAH, Ni and Pb (Pb-to-PAH, Ni-to-PAH, Pb-to-Ni) are observed. The variability in their ratios means that the composition and the aggregate source profiles of industrial emissions influencing the Marseille area change substantially from day to day, presumably because of the variable processes applied in the industrial area. For example, enrichment in elemental Pb relative to Ni and PAH is often observed and could be explained by increasing inputs from steel manufacturing emissions. In addition, ambient ratios of Ni-to-PAH fall between the characteristic ratios of HFO combustion and coke production, suggesting a mixing between these two sources. These observations serve to illustrate that the concentrations of the markers are governed by several and non-constant processes that cannot be represented by a single source class profile in the CMB model. As a result, along with non-industrial source profiles (see Sect. 2.3) three source profiles representative of the major regional industrial processes and of the emissions as detected at the receptor site (Fig. 4) are included simultaneously in the CMB model: metallurgical coke production (Weitkamp et al., 2005), HFO combustion/shipping (Agrawal et al., 2008), and steel manufacturing (Tsai et al., 2007). Thereby, CMB determines for each

sample a weighted average contribution of the three different profiles, which ultimately better constrains the amount of industrial OC compared to estimates based on a single source profile, the omission of metallurgical coke production, HFO combustion or steel manufacturing leads to an underestimation by the model for concentrations of PAH, V, Ni, and Pb, respectively. Therefore, the sum of contributions from these three sources will be considered as our best estimate for industrial emissions and will be referred to as "total industrial" in the following discussions.

3.3 Quality control

Statistical performance measures usually used in the CMB modelling as a quality control check of the CMB calculation generally includes the use of R-square (target 0.8–1.0), chi-square (target 0–4.0), t-test (target >2) and the absence of cluster sources (Watson et al., 1998). The CMB solutions presented here meet these 4 criteria for all of the samples. Another requirement for a good fit is the marker's calculated-to-measured ratios (C/M) with a target value that we fixed between 0.75 and 1.25 in order to provide reasonable bounds on CMB results. Marker C/M ratios are represented in Fig. 5. Concentrations of alkanes, PAH, levoglucosan, V, and Pb are well estimated by the model. In contrast, hopanes and EC concentrations are overestimated and underestimated, respectively, for roughly one-fifth of the samples. These discrepancies can probably be assigned to chemical degradation of hopanes (see Sect. 4.4.1). Finally, Ni concentrations are systematically underestimated by the model, with a median C/M ratio of 0.8. This underestimation can most likely be assigned either to the presence of unaccounted Ni sources or to the fact that the profile of HFO combustion from shipping emissions may not be representative of all heavy fuel combustion emissions such as those occurring at industrial boilers. However, on a general basis, all the markers are reasonably represented by the CMB model using this specific combination of source profiles and fitting species. Although the industrial source profiles tested here were not determined for French emissions, they seem to reflect satisfactorily the emissions in this area.

4 Results and discussions

4.1 PM$_{2.5}$ overall composition

Figure 6 presents the PM$_{2.5}$ average chemical mass balance over the entire sampling period. The dataset (average, min and max) that enabled the construction of this mass balance is provided in the supplementary information (Tables S1, S2 and S3). The Organic Matter fraction (OM) is calculated according to an OM-to-OC conversion factor of 1.67, inferred from the comparison between AMS (aerosol mass spectrometer) and LPI (Dekati 13-stage low pressure cascade impactor) measurements of OC in the PM$_1$ fraction on a daily
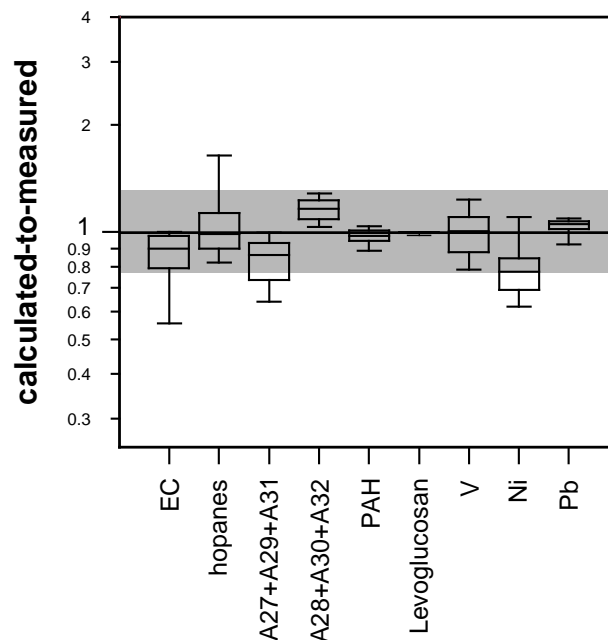

Fig. 5. Model output quality control: comparison between the measured and the calculated concentration of different markers included in CMB modelling: EC, hopanes (sum of 17α(H)-trisnorhopane, 17α(H),21β(H)-norhopane, 17α(H),21β(H)-hopane and 22S,17α(H), 21β(H)-homohopane), odd carbon number alkanes (A27+A29+A31), even carbon number alkanes (A28+A30+A32), PAH (sum of benzo[b,k]fluoranthene, benzo[e]pyrene, indeno[1,2,3-cd]pyrene and benzo[ghi]perylene), levoglucosan, V, Ni and Pb. Black line denotes the 1:1 line and grey area delimit the 0.75–1.25 range.

basis (data not shown). This value suggests a relatively high contribution of oxygenated OM, as previous studies reported OM-to-OC conversion factor ranging from 1.3 for freshly emitted anthropogenic OM up to 2 for highly oxidized OM (Aiken et al., 2008). Independently on the air masses circulation, carbonaceous matter represents constantly the dominant fraction of PM mass, with OM and EC accounting on average for 54% and 9.5% of the total PM mass, respectively. Water soluble organic carbon (WSOC) contributes to 47% of OC on average, which is consistent with the relatively high OM-to-OC ratio ($\sim$1.7).

Among inorganic components, ammonium sulphate largely dominates (by a ratio of 6) over ammonium nitrate. Ammonium nitrate exhibits a remarkable diurnal variation with higher contributions during nighttime (3.4% in daytime against 5% in nighttime). This diurnal pattern is most probably related to modifications in the partitioning conditions between the gas and particulate phases. Finally, it is worthwhile to note that the 108 quantified organic compounds account for only 4% of the total organic mass (Table S3, Supplement). Even though this identified fraction is on average dominated by carboxylic acids and phthalate esters, this
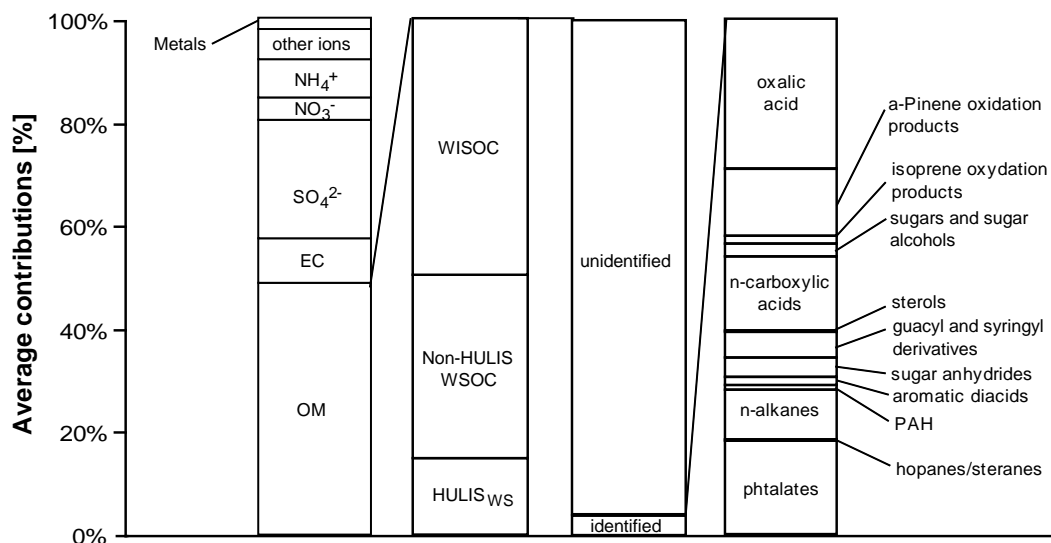
Fig. 6. PM$_{2.5}$ average chemical mass balance, over the entire period of study. For HULIS$_{WS}$ (Water Soluble Humic LIke Substances), a pinene and isoprene oxidation products see El Haddad et al. (2011).

average mass balance encompasses a high variability in the temporal trends of the different components.

4.2   Primary source contributions assessed by the CMB

Figure 7a represents the time series of source contribution estimates obtained by the CMB. Among the sources considered here, vehicular emission is the dominant source of primary OC during the whole sampling period, accounting on average for 17% of the total mass (Fig. 7a). Vegetative detritus and biomass burning are minor sources, contributing to 2.0% and 0.8% of the total OC, respectively. Even though profile representative of natural gas combustion emissions was included in the CMB analysis, the contributions from this source computed by CMB were not significantly different from 0.

Total industrial emissions contribute on average for 2.3% of the total OC mass. Their relative contribution does not exceed 7% even on events ascribed to industrial emissions. Assuming that emissions from heavy fuel oil combustion are entirely ascribed to shipping (very small contribution from industrial boilers), CMB estimates for this emission source contribute on average for 1.2% of the total OC. Although shipping contributions may appear low in an environment such as Marseille, our results are in good agreement with CMB source apportionments near the Los Angeles-Long Beach harbour (the busiest port in the US) reporting shipping contributions lower than 5% (Minguillon et al., 2008).

Albeit their relatively low contributions to OC, during industrial events, SMPS measurements show very sharp bursts of particles smaller than 80 nm associated with increases in SO$_2$ concentrations (Fig. 8). Even if the total concentration of submicron particles (11–1000 nm) can reach up to

10^5 cm^{-3} over Marseille during industrial events, these particles do not contribute significantly to the total mass. In terms of total submicron particle number, the influence of industrial emissions over Marseille can be roughly assessed by isolating these specific industrial events from urban background particle number concentrations. Industrial particle events were defined according to SO$_2$, PAH and metals concentration levels, and local wind direction associated with MM5 wind field's forecasts. The submicron particle number average concentration is 19 300 cm^{-3} during the whole field campaign period. Excluding the industrial events periods, this average concentration decreases to 14 100 cm^{-3}. Consequently the impact of industrial events on the total submicron particles number can be estimated to about 27%, almost 10 times higher than the impact on OC mass concentrations. Moreover, industrial emissions dominate the ambient concentrations of heavy metal and PAH (Fig. S1 in the Supplement), which is a noteworthy result as in urban areas PAH are usually attributed by CMB to vehicular emissions, in absence of biomass burning (Schauer and Cass, 2000) or coal combustion (Rutter et al., 2009).

A final key point highlighted in Fig. 7a is that the aggregate contributions from primary sources represents on average only 22 ± 5% of OC. As a result, the majority (∼78%) of the OC remains un-apportioned (Fig. 7a). Under-apportionment of ambient OC by CMB modelling has often been reported for summertime measurements (Subramanian et al., 2007; Zheng et al., 2006) and the un-apportioned fraction is classically associated with SOA. This fraction will be subsequently referred to as "CMB SOC". The high contribution of the CMB SOC fraction observed here is consistent with the preliminary PCA analyses (see Sect. 3.1). However, because
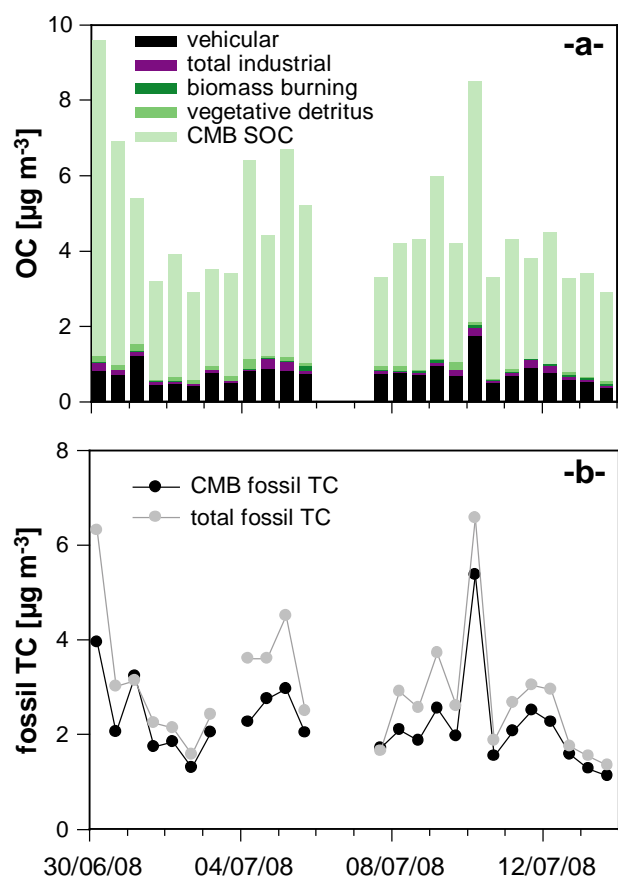
Fig. 7. (a) Source contributions to ambient organic carbon (OC) determined by the CMB modelling. **(b)** Comparison of TC fossil fractions resolved by ^{14}C and CMB modelling (sum of TC (OC+EC) emitted from mobile sources and industrial sources).

CMB SOC is an indirect apportionment, its contribution is likely to be impacted by a number of implicit parameters that underlie the CMB analysis, such as the choice of source profiles, missing sources, chemical degradation of organic markers or various artifacts. These different parameters are further investigated in Sects. 4.3 and 4.4.

4.3 Comparison with ^{14}C

In order to constrain the CMB model outputs, radiocarbon content of carbonaceous aerosol (^{14}C) can be used as a very valuable and interesting tool. ^{14}C measurements enable a direct and quantitative distinction between fossil and modern sources (Bench, 2004; Gustafsson et al., 2009; Szidat et al., 2004; Tanner et al., 2004). The central idea is that modern carbonaceous materials arising for example from biomass burning or biogenic emissions includes a constant level of ^{14}C in equilibrium with current ^{14}CO$_2$ concentrations formed from interactions of cosmic rays with atmospheric nitrogen. In contrast, carbonaceous aerosol emitted from the combustion of fossil fuel, oil or coal feedstock

whose age much exceeds the half life of ^{14}C, are radiocarbon free. This fraction is often referred to as fossil carbon. In practice, the modern signal determined by this technique is complicated by the atmospheric thermonuclear weapon tests in the late 1950s that have doubled the radiocarbon content of the atmosphere in the Northern Hemisphere (Levin et al., 1985). Since the cessation of these testing, atmospheric ^{14}C content has declined as this excess is mixed into the biosphere. Consequently, ^{14}C/^{12}C ratio relative to (^{14}C/^{12}C)$_{1950}$ ratio before nuclear tests (i.e., (^{14}C/^{12}C)-to-(^{14}C/^{12}C)$_{1950}$) is dependent on the age of the emitting plants, as biomass photosynthesized 30, 20, 10, and 0 yr before the FORMES study (in 2008) would have a ratio of 1.35, 1.18, 1.11, and 1.05, respectively (Levin et al., 2010). As a result, the present atmospheric modern fraction lies still slightly over the reference value of before 1950 (ratio of 1.05), but values characteristic of biomass burning aerosol are significantly higher (burned trees were harvested long before 2008), which complicates the choice of this ratio. However, as biomass burning constitute, in our case, a minor source, the isotopic signal of the collected organic aerosol is expected to have a ratio close to the current ratio. Here, we have chosen the low value of 1.1 for this ratio, a value that is usually used in source apportionment studies using ^{14}C data (Ding et al., 2008; Zheng et al., 2006). Consequently, in order to get the contemporary fraction (f_C), the modern fraction (f_m) is divided by the aforementioned ratio of 1.1; this corrected value is subsequently subtracted to 1 in order to obtain the fossil fraction (f_f).

The source increments assessed by the CMB are compared with ^{14}C results in Fig. 7b. The latter approach apportions the fossil and contemporary fractions of carbon that can be oxidized at 850 °C under oxygen, thus, denoting the total carbon (EC + OC). For comparison purposes, sources resolved by the CMB approach are further classified into two categories as having fossil or modern origins. Fossil sources consist of total carbon from vehicular emissions, industrial emissions and natural gas combustion, whereas modern sources include wood combustion and vegetative detritus. For each source type, the CMB apportioned EC is added to the apportioned OC to get the total carbon. Figure 7b illustrates the estimate of total fossil carbon obtained by the two independent methods (^{14}C and CMB). A strong correlation exists between the two approaches (R^2 = 0.87, n = 23), underscoring the proper choices in the selected sources and profiles. The quasi-systematic difference (∼28%) between the two methods can most likely be related to SOA from fossil origins but also with the other sources of uncertainties in the CMB (like chemical degradation of organic markers or missing primary sources). However, the very good agreement between the two methods highlights that the uncertainties related to assumptions underlying the CMB approach does not significantly affect the different primary sources contributions.
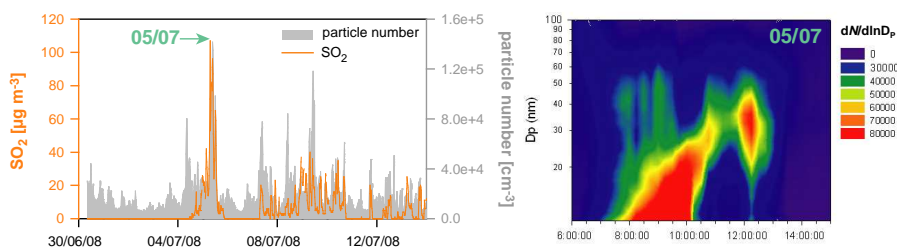
Fig. 8. Time series over the sampling period of SO$_2$ [µg m^{-3}] and particle total number [cm^{-3}] measured using a SMPS (11–1000 nm). The evolution of particle distribution is also illustrated in the case of 5 July, when the sampling site was downwind of the industrial area (see Fig. 3).

4.4 CMB un-apportioned OC and associated uncertainties

4.4.1 Evidence of chemical degradation of hopanes

Figure 9 presents time series of the concentrations for the main vehicular markers: EC and the sum of the three most predominant hopanes (17α(H),21β(H)-norhopane, 17α(H),21β(H)-hopane and 22S,17α(H), 21β(H)-homohopane). In urban locations, concentrations of these markers are dominated by mobile sources (Stone et al., 2008; Subramanian et al., 2007 and references therein). However, these markers can be emitted from other anthropogenic sources, mainly hot asphalt uses (Rogge et al., 1997b), coal combustion (Oros and Simoneit, 2000; Zhang et al., 2008), HFO combustion (Rogge et al., 1997a) and metallurgical coke production (Weitkamp et al., 2005). Biomass burning from residential heating in winter can also represent a substantial source of EC but not of hopanes (Favez et al., 2010). During the period of our study, the ambient concentrations of hopanes and EC vary by a factor of five, with no clear pattern. This variability reflects, once again, the strong influence that meteorological conditions and/or other factors have upon PM constituents in Marseille.

Hereafter, ambient ratios between vehicular emissions markers are investigated, in order to remove the influence from meteorological factors and try to reveal influences from photochemical aging or mixing of the vehicular emissions with other emissions. The central idea is that at the point of emission there are characteristic ratios between molecular markers. At a receptor site, the ambient concentration ratios between the markers can evolve with distance downwind due to the mixing of emissions from different sources and to photochemical processing as more reactive markers are preferentially oxidized. The first approach involves the construction of scatter plots between the concentrations of these markers (data not shown). Scatter plots that organize along a straight line point to the predominance of a single source. The slope corresponds to the marker ratio characteristic of the predominant source. For comparison between ambient and emission ratios, the marker ratios characteristic of vehicular emis-
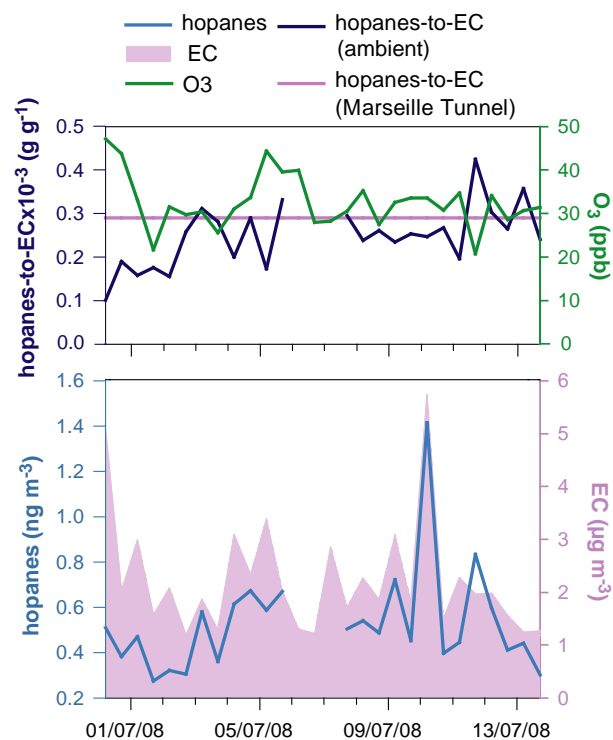

Fig. 9. Time series of EC and sum of hopane (17α(H)-21β(H)-norhopane, 17α(H)-21β(H)-hopane and 17α(H)-21β(H)-22S-homohopane). The Ambient concentration ratios of Hopanes-to-EC observed at Marseille (dark blue) are compared to the ratio specific of vehicular emissions in France (green) (El Haddad et al., 2009). Ozone mixing ratio is also plotted as a surrogate for photochemical activity. The hopane-to-EC ratios and O$_3$ show negative correlation consistent with hopane oxidation.

sions in France are drawn from a previous tunnel experiment conducted in Marseille (El Haddad et al., 2009). First, scatter plots between the different hopanes are considered. The result shows a good correlation between these markers ($R^2 > 0.9$, $n = 26$), with slopes corresponding to the ratios at the point of emission, supporting that ambient concentrations of hopanes are dominated by the emissions of mobile

sources. In contrast, hopanes concentrations are poorly correlated to EC concentrations ($R^2 = 0.65$, $n = 26$), which can result from: (i) other unconsidered sources of EC, (ii) variability in the ratio of vehicular emissions or (iii) the photochemical degradation of the markers. In order to address this issue, the ambient ratios between the sum of hopanes and EC, which is supposed to be a non-reactive marker, are compared to the ratio at the emission (El Haddad et al., 2009) (Fig. 9). Also shown is the time series of ozone concentrations, used as a surrogate to photochemical activity. Some extent of decrease in the hopanes-to-EC ratios can be noticed during periods characterised by high ozone concentrations, pointing to hopane oxidation.

In order to rule out any potential influence from mixing of vehicular emissions with other EC sources which could also explain the observed depletion in hopanes-to-EC ratios, a ratio-ratio approach is used to provide a clearer picture (Fig. 10). This approach was previously used in conjunction with CMB modelling in order to visualize source mixing and photochemical aging (Robinson et al., 2006a, b, c, d). The core of this approach entails the construction of scatter plots of ratios between three markers: two target markers (17α(H),21β(H)-norhopane and 17α(H),21β(H)-hopane) whose concentrations are normalized by the same reference marker (EC). These ratios are displayed in Fig. 10 for ambient data and for the emission sources of EC and hopanes stated above. The source profile appears as a point on the ratio-ratio plot. Therefore, ambient data that cluster to a single point imply the predominance of a single source for the selected markers. In contrast, ambient data that fall on a line between two source profiles indicate the existence of two sources with varying source strengths (Robinson et al., 2006a). As shown in Fig. 10, ambient data spread along a line that emanates from the French vehicular emission point located in the upper right hand of the ambient data points. This observation can be interpreted by a mixing scenario between vehicular sources and sources with suspected smaller hopanes-to-EC ratios, such as HFO combustion and coke production. Nevertheless, Fig. 10 shows that, during days with large concentrations of PAH (hence, with large influences of emissions linked to HFO and coke production), the ratios still cluster around that of vehicular emissions, an indication that these former sources do not modify significantly the ratios between markers. Conversely, a significant depletion (factor-of-three) of hopanes-to-EC ratios is associated with high concentrations of sulphate and ozone (Fig. 10b and c), surrogates to photochemical activity. Such a scenario suggests that there is a relatively stable chemical profile for the emission of mobile sources consistent with the profile established by El Haddad et al. (2009) and that oxidation reduces the ratio to different levels along a roughly 1:1 line. The length of this line increases with photochemical aging. This is consistent with Robinson et al. (2006) findings, reporting a seasonal variation in hopanes-to-EC ratios by comparing monthly average data in Pittsburgh, US (Robinson et al.,
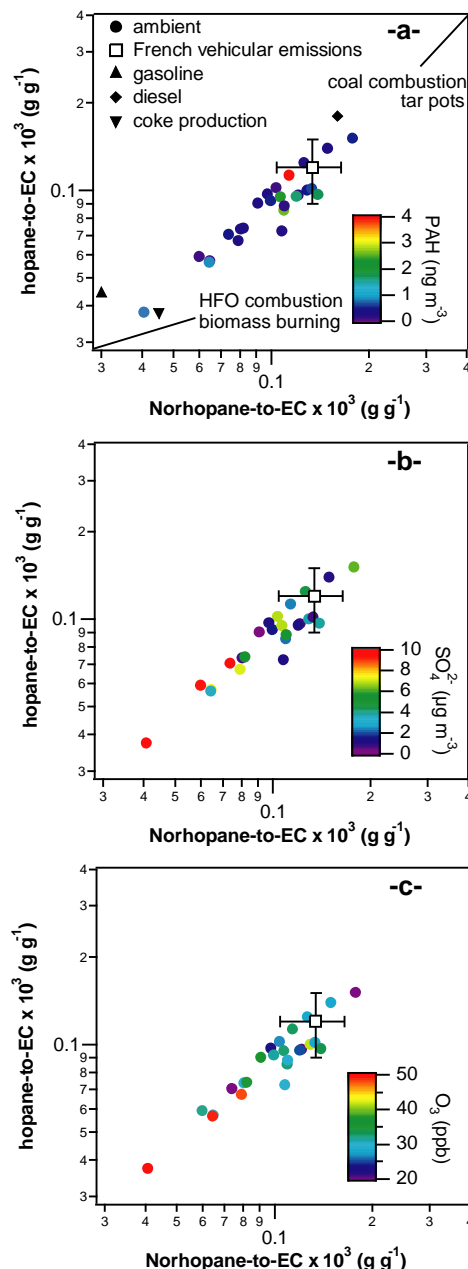

Fig. 10. Ratio-ratio plot of 17α(H)-21β(H)-norhopane and 17α(H)-21β(H)-hopane normalized by EC for the ambient data in Marseille. Colours of ambient data scatter plot denote the concentration levels of **(a)** PAH (sum of: benzo[b,k]fluoranthene, benzo[e]pyrene, indeno[1,2,3-cd]pyrene and benzo[ghi]perylene) (ng m^{-3}), **(b)** inorganic sulfate (μg m^{-3}) and **(c)** ozone (ppb). Also shown are emission ratios for different sources of hopanes and EC, including: French vehicular emissions (El Haddad et al., 2009), gasoline catalyst vehicles (Schauer et al., 2002), diesel vehicles (Schauer et al., 1999), coke production (Weitkamp et al., 2005), coal combustion (Oros and Simoneit, 2000; Zhang et al., 2008), tar pots (Rogge et al., 1997a), and HFO combustion (Rogge et al., 1997b). Arrows point to sources that do not fall within the bounds of the plot.

2006a). In Figs. 9 and 10, the clear anti-correlation between the hopanes-to-EC ratios and the ozone levels highlights a fast photochemical aging of these markers, also supporting the results from laboratory measurements of the oxidation of molecular markers from vehicular emissions (Weitkamp et al., 2008).

Decay of hopanes transgresses one of the underlying assumptions of CMB modelling, a consequence being an underestimation of the contribution from fresh vehicular emissions to ambient OC. This underestimation can be roughly evaluated with the magnitude of the depletion in the ambient hopanes-to-EC ratios relative to emission ratio; this depletion ranges between 1 and 2.5 with an average of 1.25 (i.e., 0 to 60% with an average of 20% for the oxidized hopanes). Based on this rough estimate, correcting the vehicular contributions to account for photochemical decay could only explain ~4% of the un-apportioned OC.

4.4.2 Positive sampling artifacts

OC measurements are often subjected to positive sampling artifacts and previous studies have proposed artifacts as a potential explanation for unexpectedly high level of un-apportioned OC (Zheng et al., 2006). Positive artifacts are associated with the adsorption of semi-volatile organic compounds (SVOC) onto the filters, leading to an overestimation of OC. Therefore, correcting the ambient OC for a positive artifact reduces the amount of "CMB SOC". However, positive artifacts also appear to be dominant artifact in emission measurements (Fine et al., 2002; Hildemann et al., 1991; Robinson et al., 2006b). The correction of positive artifact in source profiles enhances marker-to-OC ratios, which decreases the amount of OC apportioned to primary sources, hence increases the un-apportioned OC. Accordingly, if the artifacts on both the source and the ambient measurements are equivalent, their effects on the un-apportioned OC will cancel out. Generally, artifacts on source samples are larger than that on ambient samples, since they are measured at higher concentrations than that prevailing in the real atmosphere (Favez et al., 2010; Subramanian et al., 2007). Consequently, correction of both source and ambient measurements for artifacts may somewhat add to the amount of the un-apportioned OC, instead of decreasing it.

Another strong piece of evidence that sampling artifacts have little influence on the un-apportioned OC is the excellent agreement between the measured (TEOM-FDMS) and the reconstructed PM mass (Fig. 12), since positive artifact would lead to an overestimation of the reconstructed PM mass. This argument clearly diminishes the probability that sampling artifacts can explain the high levels of un-apportioned OC.

4.4.3 Other primary sources

In this study, the CMB analysis accounts for the major primary sources, including motor vehicles, industries and biomass combustion. However, the fact that a major fraction of OC remains unaccounted for raises the possibility that other primary sources may be significant. The large dataset of ambient organic compounds quantified in this study provides the opportunity to evaluate the influence of other primary sources, albeit without being able to propose a reliable estimate of their contributions.

First, we can consider the concentrations and trends of phthalate esters (Fig. 11a). These compounds, commonly associated with adverse health effects, are widely used as plasticizers in several polymeric materials (Staples et al., 1997). They are frequently used in construction materials, paint pigments, caulk, adhesives and lubricants (Staples et al., 1997). Following their universal uses, these additives are now ubiquitous in the atmosphere, to which they are released via two possible pathways: (i) they are emitted by migration within the polymeric matrix and subsequent exudation and volatilization; in this case, their emission rate increases with ambient temperature (Staples et al., 1997). (ii) They are also emitted during the incineration of plastic materials (Simoneit et al., 2005). Four phthalate esters are detected in our study, with diisobutyl phthalate being the dominant constituent (concentration range 6.79–69.4 ng m^{-3}), followed by bis(2-ethylhexyl) and di-n-butyl phthalates (Table 1). Benzyl n-butyl phthalate was the less abundant constituent with concentrations ranging between 0.107 and 3.85 ng m^{-3}. Although phthalate esters are one of the most dominant chemical class in the aerosol during the period of study, their contribution to the overall OC mass balance ($<1\%$) is substantially smaller than the amount of un-apportioned OC. In the same way as bis(2-ethylhexyl)phthalate represented in Fig. 11a, phthalate esters show a good correlation with OC, suggesting diffuse emission sources rather than a point source such as incineration emissions. In addition, the contribution of bis(2-ethylhexyl)phthalate to the OM mass increases with the ambient temperature (Fig. 11b), suggesting an increase of its emission rate with the temperature. These observations are in line with the first emission pathway mentioned above.

Second, we can consider the concentrations of sugars and their derivatives in the aerosol of Marseille (Table 1). Recent studies indicate that these compounds can contribute significantly to the water soluble fraction of OA and suggest that they are mainly emitted from primary biogenic sources including pollen, bacteria, fungal spores and the re-suspension of soil biota (Bauer et al., 2008; Ion et al., 2005; Kourtchev et al., 2008; Medeiros et al., 2006; Wang et al., 2008; Yttri et al., 2007). In Marseille, sugar contribution to OC is significantly lower than those reported in other studies, mostly conducted in forested environments (for comparison see supplement Table S4). Bauer et al. (2008) propose mannitol and arabitol as specific markers for the quantification of fungal
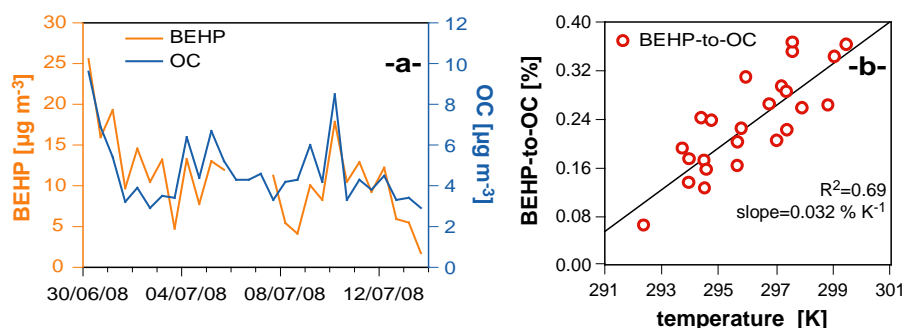
Fig. 11. BEHP (Bis(2-ethylhexyl) phthalate; plasticizer mostly in the particulate phase) trends during the period of study: **(a)** time series of BEHP and OC; good correlation between the two components is observed ($R^2 = 0.73$). **(b)** Scatter plot of BEHP contribution to the organic carbon (%) versus temperature (K). The contribution of BEHP increases with temperature which underscore that its emission proceeds via evaporation from the polymeric matrix.

Table 2. Pearson correlation coefficients (R^2, $N = 26$) between biogenic markers, vegetative detritus OC and CMB SOC. $0.5 < R^2 < 0.8$ and $R^2 > 0.8$ are displayed, respectively, in bold character and in bold character and underlined.

R^2	Glucose	fructose	arabitol	mannitol	sucrose	trehalose	veg. detritus	CMB SOC
glucose	1	**0.64**	0.24	0.15	**0.72**	0.34	0.01	0.02
fructose		1	**0.59**	**0.52**	**0.70**	**0.51**	0.01	0.01
arabitol			1	**_0.92_**	0.14	0.37	0.02	0.01
mannitol				1	0.10	0.44	0.02	0.01
sucrose					1	0.34	0.01	0.03
trehalose						1	0.01	0.02
veg. detritus							1	0.21
CMB SOC								1

spore contribution to organic carbon. Considering the ratio of OC-to-(mannitol + arabitol) of 4.5 reported in Bauer et al. (2008), the contribution of fungal spores can be estimated, in our case, at only 0.1% of OC on average. To date, there is a paucity of studies that provide a quantitative estimation of the overall contribution from primary biogenic emissions to OC. On the basis of the dataset obtained within the CARBOSOL project, Gelencser et al. (2007) estimate that these sources contribute on average to 3% of the TC, using the cellulose as a marker present in every biological aerosol (Gelencser et al., 2007). More recently, integrating the sugars and their derivatives into a PMF model, Jia et al. (2010) report a contribution of 4% and 9% from biological aerosol to the total PM$_{2.5}$ mass in a rural and an urban sites, respectively. In the present study, we used a multiple correlation approach in order to elucidate the sugar origins and their influence on OC concentrations in Marseille. The results are reported in Table 2. The low correlation coefficients ($R^2 < 0.72$, $n = 26$) between the different sugars imply that their emissions in the atmosphere most likely involve several sources. These sources seem to be, moreover, different from those involved in the emissions from leaf surface waxes and plant detritus, given the very low correlation coefficients between sugars and biogenic n-

alkanes (Table 2). Finally, the very low correlations observed between these compounds and "CMB SOC" suggest that the primary biogenic materials do not contribute significantly to the un-apportioned fraction of OC, consistent with the findings reported in previous studies (Gelencser et al., 2007; Jia et al., 2010).

In this section, we showed that it is very unlikely that some of the other known primary sources of OC can contribute significantly to the OC pool in our measurements. Thus, we can hypothesize that the large amount of un-apportioned OC (78% of the overall OC mass) could mostly be attributed to secondary organic carbon (SOC). Therefore, CMB SOC represents a higher estimate of SOC in the OC mass balance. This secondary fraction of OC is discussed in detail in the companion paper (El Haddad et al., 2011).

4.5 Source contributions to fine-particle mass

In order to determine the contributions from primary sources to PM$_{2.5}$ mass, OM mass associated with each source is calculated applying an OM-to-OC conversion factor specific for each source; the result is then combined with the corresponding EC, sulphate, nitrate and ammonium concentrations, as given in the source profiles. Then, secondary sulphate, nitrate
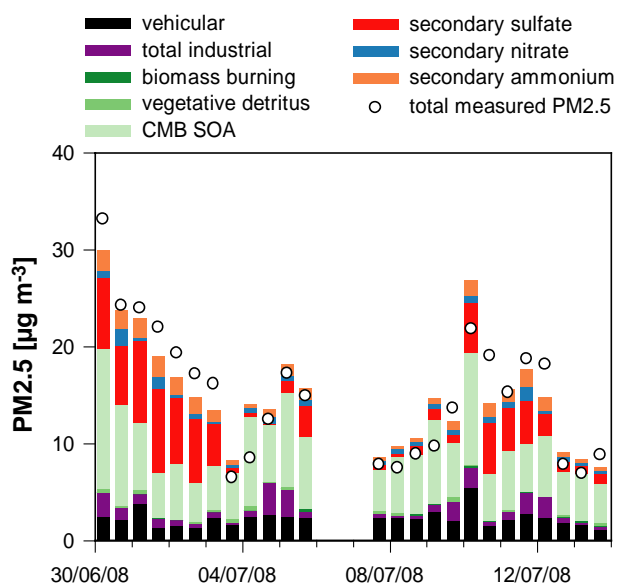
Fig. 12. Source contributions to fine particulate matter (PM$_{2.5}$) estimated by CMB modelling. Also shown are the concentrations of PM$_{2.5}$ measured by TEOM-FDMS (white circles).

and ammonium are deduced by subtracting from the measured ionic species the primary emissions of these species. The OM-to-OC conversion factors applied here are 1.2 for vehicular emissions, industrial emissions, and natural gas combustion (based on Aiken et al., 2008 and Mohr et al., 2009), 1.7 for biomass burning (based on Puxbaum et al., 2007 and references therein), and 2.0 for vegetative detritus (based on Kunit and Puxbaum, 1996). The difference between the total OM, determined by applying an OM-to-OC conversion factor of 1.67 to total OC (see Sect. 4.1), and the apportioned OM attributed to primary sources represents the "CMB SOA". When comparing CMB SOA to the CMB SOC, an OM-to-OC factor of 1.82 could be inferred, which is consistent with the secondary origin of the CMB SOA fraction (Aiken et al., 2008).

Figure 12 shows a time series of the ambient PM$_{2.5}$ mass apportioned by CMB. Primary sources considered by CMB contribute only to a small fraction of the ambient PM$_{2.5}$. For example, the average contributions to total PM mass from motor vehicles, industries, vegetative detritus and biomass burning are 17, 7.1, 1.6 and 0.52%, respectively. Such estimates for the aggregate contributions of primary sources of PM$_{2.5}$ ($\sim$26% on average) fall towards the low end of the range of previous CMB modelling studies performed in urban areas (e.g., Ke et al., 2007; Stone et al., 2008; Zheng et al., 2006). Contribution of geological dust and sea salt are not represented in the Fig. 12. However, considering Al as a marker of urban dust and a PM-to-Al ratio of 10 (Chow et al., 2003), this contribution can be estimated on average at 2% of total PM$_{2.5}$ (0.35 µg m^{-3} of dust). Such contributions of dust are almost by one order of magnitude lower than con-

tributions observed in other urban European site (Querol et al., 2008; Sillanpää et al., 2005) such as Barcelona or Athens (2–3 µg m^{-3} of dust). These large discrepancies might be assigned to the meteorological conditions encountered during the sampling period as no severe dust episodes were encountered in our case. Likewise, based on Na$^+$ concentrations (Virkkula et al., 2006), sea salt can be estimated to contribute between 0.08% and 6.4% (average 1.3%) of the total PM$_{2.5}$ mass, following the method reported in Virkkula et al. (2006). The most important conclusion is that ambient PM$_{2.5}$ concentrations are governed by secondary species in our case. Un-apportioned organic PM (CMB SOA), much of which is likely SOA, is the largest contributor (43%), followed by inorganic ions of secondary origins that account on average for 31% of the PM mass. The importance of the contribution from secondary components to the ambient PM is even more pronounced when high-concentration days are considered, especially at the beginning of the study (days associated with local wind motions).

5   Conclusions

This paper presents CMB analysis of organic molecular marker data to investigate the primary sources of organic aerosol in Marseille environment that is impacted by severe photochemical activity combined with a complex mixture of primary sources, including fugitive industrial emissions and shipping. This kind of emissions had been rarely considered before in CMB modelling studies and their impacts on the aerosol components still not constrained at all. We have demonstrated that PAH, Ni, V and Pb can be used as markers for industrial emissions and in order to fully represent the industrial processes we injected in the CMB three source profiles representative of the main processes in Marseille (HFO combustion, metal smelting and coke production).

Primary OC estimated by the CMB model used here contributes on average for only 22% and is dominated by the vehicular emissions ($\sim$17%). The main conclusion highlighted by this CMB analysis is that industrial and shipping emissions contribute on average for only 2.3% of the total OC (7% of PM$_{2.5}$), but they dominate the concentrations of PAH and heavy metals, and are associated with bursts of submicron particles. This is a noteworthy result as, for instance, in urban areas PAH are usually attributed by CMB to vehicular emissions (gasoline ones), when industrial sources are not included. Consequently the omission of industrial emissions in areas heavily impacted by such sources would lead to substantial uncertainties in the CMB analysis, hindering accurate estimation of non-industrial primary sources and secondary sources. This result implies that CMB modelling should not be a straightforward exercise and one has to carefully investigate the marker behaviours and trends beforehand, especially in complex environments such as Marseille. From a health impact point of view, being associated

with bursts of submicron particles and carcinogenic and mutagenic components such as PAH, these emissions are most likely related to negative health outcomes and should be regulated despite their small contributions to OC. Finally, the good agreement between CMB source increments and those apportioned by ^{14}C suggest that the industrial source profiles used in this study reflect satisfactorily the emissions in Marseille although these were not determined for French emissions. Thus, the profiles tested here can be most likely used to apportion such sources in other urban areas heavily impacted by industrial and shipping emissions.

Another key point highlighted in this study is that 78% of OC mass cannot be attributed to the major primary sources and thus remains un-apportioned. While clear evidence of photochemical decay of molecular markers (mainly hopane homologues) have been revealed, this decay does not appear to significantly alter the CMB estimates of the total primary OC. Sampling artifacts and unaccounted primary sources also appear to marginally influence the amount of un-apportioned OC. Therefore, this significant amount of un-apportioned OC is mostly attributed to secondary organic carbon. This conclusion contributes to the growing body of evidence that the secondary fraction of the organic aerosol dominates the summertime ambient concentrations even in urban areas and fosters the importance of controlling strategies focusing on precursor emissions.

Supplementary material related to this article is available online at: http://www.atmos-chem-phys.net/11/2039/2011/ acp-11-2039-2011-supplement.pdf.

References

Agrawal, H., Welch, W. A., Miller, J. W., and Cocker, D. R.: Emission measurements from a crude oil tanker at sea, Environ. Sci. Technol., 42, 7098–7103, 2008.

Aiken, A. C., DeCarlo, P. F., Kroll, J. H., Worsnop, D. R., Huffman, J. A., Docherty, K. S., Ulbrich, I. M., Mohr, C., Kimmel, J. R., Sueper, D., Sun, Y., Zhang, Q., Trimborn, A., Northway, M., Ziemann, P. J., Canagaratna, M. R., Onasch, T. B., Alfarra, M. R., Prevot, A. S. H., Dommen, J., Duplissy, J., Metzger, A., Baltensperger, U., and Jimenez, J. L.: O/C and OM/OC Ratios of Primary, Secondary, and Ambient Organic Aerosols with High-Resolution Time-of-Flight Aerosol Mass Spectrometry, Environ. Sci. Technol., 42, 4478–4485, doi:10.1021/es703009q, 2008.

Bauer, H., Claeys, M., Vermeylen, R., Schueller, E., Weinke, G., Berger, A., and Puxbaum, H.: Arabitol and mannitol as tracers for the quantification of airborne fungal spores, Atmos. Environ., 42, 588–593, 2008.

Bench, G.: Measurement of contemporary and fossil carbon contents of PM$_{2.5}$ aerosols: Results from Turtleback Dome, Yosemite National Park, Environ. Sci. Technol., 38, 2424–2427, 2004.

Birch, M. E. and Cary, R. A.: Elemental carbon-based method for monitoring occupational exposures to particulate diesel exhaust, Aerosol Sci. Technol., 25, 221–241, 1996.

Cachier, H., Aulagnier, F., Sarda, R., Gautier, F., Masclet, P., Besombes, J. L., Marchand, N., Despiau, S., Croci, D., Mallet, M., Laj, P., Marinoni, A., Deveau, P. A., Roger, J. C., Putaud, J. P., Van Dingenen, R., Dell'Acqua, A., Viidanoja, J., Santos, S. M. D., Liousse, C., Cousin, F., Rosset, R., Gardrat, E., and Galy-Lacaux, C.: Aerosol studies during the ESCOMPTE experiment: an overview, Atmos. Res., 74, 547–563, 2005.

Chauvel, C., Bureau, S., and Poggi, C.: Comprehensive chemical and isotopic analyses of basalt and sediment reference materials, Geostand. Geoanalyt. Res., 35, 125–143, doi:10.1111/j.1751-908X.2010.00086., 2010.

Chow, J. C., Watson, J. G., Ashbaugh, L. L., and Magliano, K. L.: Similarities and differences in PM$_{10}$ chemical source profiles for geological dust from the San Joaquin Valley, California, Atmos. Environ., 37, 1317–1340, 2003.

Chow, J. C., Watson, J. G., Lowenthal, D. H., Chen, L. W. A., Zielinska, B., Mazzoleni, L. R., and Magliano, K. L.: Evaluation of organic markers for chemical mass balance source apportionment at the Fresno Supersite, Atmos. Chem. Phys., 7, 1741–1754, doi:10.5194/acp-7-1741-2007, 2007.

Ding, X., Zheng, M., Edgerton, E. S., Jansen, J. J., and Wang, X. M.: Contemporary or Fossil Origin: Split of Estimated Secondary Organic Carbon in the Southeastern United States, Environ. Sci. Technol., 42, 9122–9128, 2008.

Docherty, K. S., Stone, E. A., Ulbrich, I. M., DeCarlo, P. F., Snyder, D. C., Schauer, J. J., Peltier, R. E., Weber, R. J., Murphy, S. M., Seinfeld, J. H., Grover, B. D., Eatough, D. J., and Jimenez, J. L.: Apportionment of Primary and Secondary Organic Aerosols in Southern California during the 2005 Study of Organic Aerosols in Riverside (SOAR-1), Environ. Sci. Technol., 42, 7655–7662, 2008.

Donahue, N. M., Robinson, A. L., Stanier, C. O., and Pandis, S. N.: Coupled partitioning, dilution, and chemical aging of semivolatile organics, Environ. Sci. Technol., 40, 2635–2643, doi:10.1021/esO52297c, 2006.

Drobinski, P., Said, F., Arteta, J., Augustin, P., Bastin, S., Brut, A., Caccia, J. L., Campistron, B., Cautenet, S., Colette, A., Coll, I., Corsmeier, U., Cros, B., Dabas, A., Delbarre, H., Dufour, A., Durand, P., Guenard, V., Hasel, M., Kalthoff, N., Kottmeier, C.,

Lasry, F., Lemonsu, A., Lohou, F., Masson, V., Menut, L., Moppert, C., Peuch, V. H., Puygrenier, V., Reitebuch, O., and Vautard, R.: Regional transport and dilution during high-pollution episodes in southern France: Summary of findings from the Field Experiment to Constraint Models of Atmospheric Pollution and Emissions Transport (ESCOMPTE), J. Geophys. Res.-Atmos., 112, D13105, doi:10.1029/2006JD007494, 2007.

El Haddad, I., Marchand, N., Dron, J., Temime-Roussel, B., Quivet, E., Wortham, H., Jaffrezo, J. L., Baduel, C., Voisin, D., Besombes, J. L., and Gille, G.: Comprehensive primary particulate organic characterization of vehicular exhaust emissions in France, Atmos. Environ., 43, 6190–6198, 2009.

El Haddad, I., Marchand, N., Temime-Roussel, B., Wortham, H., Piot, C., Besombes, J.-L., Baduel, C., Voisin, D., Armengaud, A., and Jaffrezo, J.-L.: Insights into the secondary fraction of the organic aerosol in a Mediterranean urban area: Marseille Atmos. Chem. Phys., 11, 2059–2079, doi:10.5194/acp-11-2059-2011, 2011.

Favez, O., El Haddad, I., Piot, C., Boréave, A., Abidi, E., Marchand, N., Jaffrezo, J.-L., Besombes, J.-L., Personnaz, M.-B., Sciare, J., Wortham, H., George, C., and D'Anna, B.: Inter-comparison of source apportionment models for the estimation of wood burning aerosols during wintertime in an Alpine city (Grenoble, France), Atmos. Chem. Phys., 10, 5295–5314, doi:10.5194/acp-10-5295-2010, 2010.

Fine, P. M., Cass, G. R., and Simoneit, B. R. T.: Chemical Characterization of Fine Particle Emissions from the Fireplace Combustion of Woods Grown in the Southern United States, Environ. Sci. Technol., 36, 1442–1451, doi:10.1021/es0108988, 2002.

Flaounas, E., Coll, I., Armengaud, A., and Schmechtig, C.: The representation of dust transport and missing urban sources as major issues for the simulation of PM episodes in a Mediterranean area, Atmos. Chem. Phys., 9, 8091–8101, doi:10.5194/acp-9-8091-2009, 2009.

Gelencser, A., May, B., Simpson, D., Sanchez-Ochoa, A., Kasper-Giebl, A., Puxbaum, H., Caseiro, A., Pio, C., and Legrand, M.: Source apportionment of PM$_{2.5}$ organic aerosol over Europe: Primary/secondary, natural/anthropogenic, and fossil/biogenic origin, J. Geophys. Res.-Atmos., 112, D23S04, doi:10.1029/2006JD008094, 2007.

Geller, M. D., Sardar, S. B., Phuleria, H., Fine, P. M., and Sioutas, C.: Measurements of particle number and mass concentrations and size distributions in a tunnel environment, Environ. Sci. Technol., 39, 8653–8663, 2005.

Grieshop, A. P., Lipsky, E. M., Pekney, N. J., Takahama, S., and Robinson, A. L.: Fine particle emission factors from vehicles in a highway tunnel: Effects of fleet composition and season, Atmos. Environ., 40, S287–S298, 2006.

Gustafsson, O., Krusa, M., Zencak, Z., Sheesley, R. J., Granat, L., Engstrom, E., Praveen, P. S., Rao, P. S. P., Leck, C., and Rodhe, H.: Brown Clouds over South Asia: Biomass or Fossil Fuel Combustion?, Science, 323, 495–498, 2009.

Hildemann, L. M., Markowski, G. R., and Cass, G. R.: Chemical composition of emissions from urban sources of fine organic aerosol, Environ. Sci. Technol., 25, 744–759, doi:10.1021/es00016a021, 1991.

Ion, A. C., Vermeylen, R., Kourtchev, I., Cafmeyer, J., Chi, X., Gelencsér, A., Maenhaut, W., and Claeys, M.: Polar organic compounds in rural PM$_{2.5}$ aerosols from K-puszta, Hungary, during

a 2003 summer field campaign: Sources and diel variations, Atmos. Chem. Phys., 5, 1805–1814, doi:10.5194/acp-5-1805-2005, 2005.

Jaffrezo, J.-L., Aymoz, G., Delaval, C., and Cozic, J.: Seasonal variations of the water soluble organic carbon mass fraction of aerosol in two valleys of the French Alps, Atmos. Chem. Phys., 5, 2809–2821, doi:10.5194/acp-5-2809-2005, 2005.

Jaffrezo, J. L., Calas, T., and Bouchet, M.: Carboxylic acids measurements with ionic chromatography, Atmos. Environ., 32, 2705–2708, 1998.

Jia, Y., Bhat, S., and Fraser, M. P.: Characterization of saccharides and other organic compounds in fine particles and the use of saccharides to track primary biologically derived carbon sources, Atmos. Environ., 44, 724–732, 2010.

Jimenez, J. L., Canagaratna, M. R., Donahue, N. M., Prevot, A. S. H., Zhang, Q., Kroll, J. H., DeCarlo, P. F., Allan, J. D., Coe, H., Ng, N. L., Aiken, A. C., Docherty, K. S., Ulbrich, I. M., Grieshop, A. P., Robinson, A. L., Duplissy, J., Smith, J. D., Wilson, K. R., Lanz, V. A., Hueglin, C., Sun, Y. L., Tian, J., Laaksonen, A., Raatikainen, T., Rautiainen, J., Vaattovaara, P., Ehn, M., Kulmala, M., Tomlinson, J. M., Collins, D. R., Cubison, M. J., Dunlea, E. J., Huffman, J. A., Onasch, T. B., Alfarra, M. R., Williams, P. I., Bower, K., Kondo, Y., Schneider, J., Drewnick, F., Borrmann, S., Weimer, S., Demerjian, K., Salcedo, D., Cottrell, L., Griffin, R., Takami, A., Miyoshi, T., Hatakeyama, S., Shimono, A., Sun, J. Y., Zhang, Y. M., Dzepina, K., Kimmel, J. R., Sueper, D., Jayne, J. T., Herndon, S. C., Trimborn, A. M., Williams, L. R., Wood, E. C., Middlebrook, A. M., Kolb, C. E., Baltensperger, U., and Worsnop, D. R.: Evolution of Organic Aerosols in the Atmosphere, Science, 326, 1525–1529, 2009.

Kanakidou, M., Seinfeld, J. H., Pandis, S. N., Barnes, I., Dentener, F. J., Facchini, M. C., Van Dingenen, R., Ervens, B., Nenes, A., Nielsen, C. J., Swietlicki, E., Putaud, J. P., Balkanski, Y., Fuzzi, S., Horth, J., Moortgat, G. K., Winterhalter, R., Myhre, C. E. L., Tsigaridis, K., Vignati, E., Stephanou, E. G., and Wilson, J.: Organic aerosol and global climate modelling: a review, Atmos. Chem. Phys., 5, 1053–1123, doi:10.5194/acp-5-1053-2005, 2005.

Ke, L., Ding, X., Tanner, R. L., Schauer, J. J., and Zheng, M.: Source contributions to carbonaceous aerosols in the Tennessee Valley Region, Atmos. Environ., 41, 8898–8923, 2007.

Kourtchev, I., Warnke, J., Maenhaut, W., Hoffmann, T., and Claeys, M.: Polar organic marker compounds in PM$_{2.5}$ aerosol from a mixed forest site in western Germany, Chemosphere, 73, 1308–1314, 2008.

Kunit, M. and Puxbaum, H.: Enzymatic determination of the cellulose content of atmospheric aerosols, Atmos. Environ., 30, 1233–1236, 1996.

Levin, I., Kromer, B., Schochfischer, H., Bruns, M., Munnich, M., Berdau, D., Vogel, J. C., and Munnich, K. O.: 25 Years of Tropospheric C-14 Observations in Central-Europe, Radiocarbon, 27, 1–19, 1985.

Levin, I., Naegler, T., Kromer, B., Diehl, M., Francey, R. J., Gomez-Pelaez, A. J., Steele, L. P., Wagenbach, D., Weller, R., and Worthy, D. E.: Observations and modelling of the global distribution and long-term trend of atmospheric 14CO(2), Tellus B, 62, 26–46, 2010.

Medeiros, P. M., Conte, M. H., Weber, J. C., and Simoneit, B. R. T.: Sugars as source indicators of biogenic organic carbon

in aerosols collected above the Howland Experimental Forest, Maine, Atmos. Environ., 40, 1694–1705, 2006.

Minguillon, M. C., Arhami, M., Schauer, J. J., and Sioutas, C.: Seasonal and spatial variations of sources of fine and quasi-ultrafine particulate matter in neighborhoods near the Los Angeles-Long Beach harbor, Atmos. Environ., 42, 7317–7328, 2008.

Mohr, C., Huffman, J. A., Cubison, M. J., Aiken, A. C., Docherty, K. S., Kimmel, J. R., Ulbrich, I. M., Hannigan, M., and Jimenez, J. L.: Characterization of Primary Organic Aerosol Emissions from Meat Cooking, Trash Burning, and Motor Vehicles with High-Resolution Aerosol Mass Spectrometry and Comparison with Ambient and Chamber Observations, Environ. Sci. Technol., 43, 2443–2449, doi:10.1021/es8011518, 2009.

Ntziachristos, L., Ning, Z., Geller, M. D., Sheesley, R. J., Schauer, J. J., and Sioutas, C.: Fine, ultrafine and nanoparticle trace element compositions near a major freeway with a high heavy-duty diesel fraction, Atmos. Environ., 41, 5684–5696, 2007.

Oros, D. R. and Simoneit, B. R. T.: Identification and emission rates of molecular tracers in coal smoke particulate matter, Fuel, 79, 515–536, 2000.

Osterberg, E., Mayewski, P., Kreutz, K., Fisher, D., Handley, M., Sneed, S., Zdanowicz, C., Zheng, J., Demuth, M., Waskiewicz, M., and Bourgeois, J.: Ice core record of rising lead pollution in the North Pacific atmosphere, Geophys. Res. Lett., 35, L05810, doi:10.1029/2007GL032680, 2008.

Petäjä, T., Kerminen, V.-M., Dal Maso, M., Junninen, H., Koponen, I. K., Hussein, T., Aalto, P. P., Andronopoulos, S., Robin, D., Hämeri, K., Bartzis, J. G., and Kulmala, M.: Submicron atmospheric aerosols in the surroundings of Marseille and Athens: physical characterization and new particle formation, Atmos. Chem. Phys., 7, 2705–2720, doi:10.5194/acp-7-2705-2007, 2007.

Pina, A. A., Villasenor, G. T., Jacinto, P. S., and Fernandez, M. M.: Scanning and transmission electron microscope of suspended lead-rich particles in the air of San Luis Potosi, Mexico, Atmos. Environ., 36, 5235–5243, 2002.

Putaud, J.-P., Raes, F., Van Dingenen, R., Brüggemann, E., Facchini, M.-C., Decesari, S., Fuzzi, S., Gehrig, R., Hüglin, C., Laj, P., Lorbeer, G., Maenhaut, W., Mihalopoulos, N., Müller, K., Querol, X., Rodriguez, S., Schneider, J., Spindler, G., Ten Brink, H., Tørseth, K., and A., W.: A European aerosol phenomenology – 2: chemical characteristics of particulate matter at kerbside, urban, rural and background sites in Europe, Atmos. Environ., 38, 889–902, 2004.

Puxbaum, H., Caseiro, A., Sanchez-Ochoa, A., Kasper-Giebl, A., Claeys, M., Gelencser, A., Legrand, M., Preunkert, S., and Pio, C.: Levoglucosan levels at background sites in Europe for assessing the impact of biomass combustion on the European aerosol background, J. Geophys. Res., 112, D23S05, doi:10.1029/2006jd008114, 2007.

Querol, X., Viana, M., Alastuey, A., Amato, F., Moreno, T., Castillo, S., Pey, J., de la Rosa, J., de la Campa, A. S., Artinano, B., Salvador, P., Dos Santos, S. G., Fernandez-Patier, R., Moreno-Grau, S., Negral, L., Minguillon, M. C., Monfort, E., Gil, J. I., Inza, A., Ortega, L. A., Santamaria, J. M., and Zabalza, J.: Source origin of trace elements in PM from regional background, urban and industrial sites of Spain, Atmos. Environ., 41, 7219–7231, 2007.

Querol, X., Alastuey, A., Moreno, T., Viana, M. M., Castillo, S.,

Pey, J., Rodriguez, S., Artinano, B., Salvador, P., Sanchez, M., Dos Santos, S. G., Garraleta, M. D. H., Fernandez-Patier, R., Moreno-Grau, S., Negral, L., Minguillon, M. C., Monfort, E., Sanz, M. J., Palomo-Marin, R., Pinilla-Gil, E., Cuevas, E., de la Rosa, J., and de la Campa, A. S.: Spatial and temporal variations in airborne particulate matter (PM$_{10}$ and PM$_{2.5}$) across Spain 1999–2005, Atmos. Environ., 42, 3964–3979, 2008.

Robinson, A. L., Donahue, N. M., and Rogge, W. F.: Photochemical oxidation and changes in molecular composition of organic aerosol in the regional context, J. Geophys. Res.-Atmos., 111, D03302, doi:10.1029/2005jd006265, 2006a.

Robinson, A. L., Subramanian, R., Donahue, N. M., Bernardo-Bricker, A., and Rogge, W. F.: Source Apportionment of Molecular Markers and Organic Aerosol. 2. Biomass Smoke, Environ. Sci. Technol., 40, 7811–7819, doi:10.1021/es060782h, 2006b.

Robinson, A. L., Subramanian, R., Donahue, N. M., Bernardo-Bricker, A., and Rogge, W. F.: Source Apportionment of Molecular Markers and Organic Aerosol. 3. Food Cooking Emissions, Environ. Sci. Technol., 40, 7820–7827, doi:10.1021/es060781p, 2006c.

Robinson, A. L., Subramanian, R., Donahue, N. M., and Rogge, W. F.: Source Apportionment of Molecular Markers and Organic Aerosol1. Polycyclic Aromatic Hydrocarbons and Methodology for Data Visualization, Environ. Sci. Technol., 40, 7803–7810, doi:10.1021/es0510414, 2006d.

Robinson, A. L., Donahue, N. M., Shrivastava, M. K., Weitkamp, E. A., Sage, A. M., Grieshop, A. P., Lane, T. E., Pierce, J. R., and Pandis, S. N.: Rethinking organic aerosols: Semivolatile emissions and photochemical aging, Science, 315, 1259–1262, doi:10.1126/science.1133061, 2007.

Rogge, W. F., Hildemann, L. M., Mazurek, M. A., Cass, G. R., and Simoneit, B. R. T.: Sources of Fine Organic Aerosol .4. Particulate Abrasion Products from Leaf Surfaces of Urban Plants, Environ. Sci. Technol., 27, 2700–2711, 1993a.

Rogge, W. F., Hildemann, L. M., Mazurek, M. A., Cass, G. R., and Simoneit, B. R. T.: Sources of Fine Organic Aerosol.5. Natural-Gas Home Appliances, Environ. Sci. Technol., 27, 2736–2744, 1993b.

Rogge, W. F., Hildemann, L. M., Mazurek, M. A., Cass, G. R., and Simoneit, B. R. T.: Sources of fine organic aerosol .8. Boilers burning No. 2 distillate fuel oil, Environ. Sci. Technol., 31, 2731–2737, 1997a.

Rogge, W. F., Hildemann, L. M., Mazurek, M. A., Cass, G. R., and Simoneit, B. R. T.: Sources of fine organic aerosol.7. Hot asphalt roofing tar pot fumes, Environ. Sci. Technol., 31, 2726–2730, 1997b.

Rolph, G. D.: Real-time Environmental Applications and Display sYstem (READY) Website (http://ready.arl.noaa.gov). NOAA Air Resources Laboratory, Silver Spring, MD, 2010.

Rutter, A. P., Snyder, D. G., Schauer, J. J., Deminter, J., and Shelton, B.: Sensitivity and Bias of Molecular Marker-Based Aerosol Source Apportionment Models to Small Contributions of Coal Combustion Soot, Environ. Sci. Technol., 43, 7770–7777, 2009.

Schauer, J. J., Rogge, W. F., Hildemann, L. M., Mazurek, M. A., Cass, G. R., and Simoneit, B. R. T.: Source apportionment of airborne particulate matter using organic compounds as tracers, Atmos. Environ. 30, 3837–3855, 1996.

Schauer, J. J., Kleeman, M. J., Cass, G. R., and Simoneit, B. R. T.: Measurement of Emissions from Air Pollution

Sources. 2. C1 through C30 Organic Compounds from Medium Duty Diesel Trucks, Environ. Sci. Technol., 33, 1578–1587, doi:10.1021/es980081n, 1999.

Schauer, J. J. and Cass, G. R.: Source Apportionment of Wintertime Gas-Phase and Particle-Phase Air Pollutants Using Organic Compounds as Tracers, Environ. Sci. Technol., 34, 1821–1832, 2000.

Schauer, J. J., Fraser, M. P., Cass, G. R., and Simoneit, B. R. T.: Source Reconciliation of Atmospheric Gas-Phase and Particle-Phase Pollutants during a Severe Photochemical Smog Episode, Environ. Sci. Technol., 36, 3806–3814, 2002a.

Schauer, J. J., Kleeman, M. J., Cass, G. R., and Simoneit, B. R. T.: Measurement of Emissions from Air Pollution Sources. 5. C1â'C32 Organic Compounds from Gasoline-Powered Motor Vehicles, Environ. Sci. Technol., 36, 1169–1180, doi:10.1021/es0108077, 2002b.

Schauer, J. J., Lough, G. C., Shafer, M. M., Christensen, W. F., Arndt, M. F., DeMinter, J. T., and Park, J.-S.: Characterization of metals emitted from motor vehicles, Res Rep Health Eff Inst, 1–76; discussion 77–88, 2006.

Schmid, H., Laskus, L., Jürgen Abraham, H., Baltensperger, U., Lavanchy, V., Bizjak, M., Burba, P., Cachier, H., Crow, D., Chow, J., Gnauk, T., Even, A., ten Brink, H. M., Giesen, K.-P., Hitzenberger, R., Hueglin, C., Maenhaut, W., Pio, C., Carvalho, A., Putaud, J.-P., Toom-Sauntry, D., and Puxbaum, H.: Results of the "carbon conference" international aerosol carbon round robin test stage I, Atmos. Environ., 35, 2111–2121, 2001.

Sheesley, R. J., Schauer, J. J., Zheng, M., and Wang, B.: Sensitivity of molecular marker-based CMB models to biomass burning source profiles, Atmos. Environ., 41, 9050–9063, 2007.

Sillanpää, M., Frey, A., Hillamo, R., Pennanen, A. S., and Salonen, R. O.: Organic, elemental and inorganic carbon in particulate matter of six urban environments in Europe, Atmos. Chem. Phys., 5, 2869–2879, doi:10.5194/acp-5-2869-2005, 2005.

Simoneit, B. R. T., Medeiros, P. M., and Didyk, B. M.: Combustion products of plastics as indicators for refuse burning in the atmosphere, Environ. Sci. Technol., 39, 6961–6970, 2005.

Staples, C. A., Peterson, D. R., Parkerton, T. F., and Adams, W. J.: The environmental fate of phthalate esters: a literature review, Chemosphere, 35, 667–749, 1997.

Stone, E. A., Snyder, D. C., Sheesley, R. J., Sullivan, A. P., Weber, R. J., and Schauer, J. J.: Source apportionment of fine organic aerosol in Mexico City during the MILAGRO experiment 2006, Atmos. Chem. Phys., 8, 1249–1259, doi:10.5194/acp-8-1249-2008, 2008.

Stuiver, M. and Polach, H. A.: Reporting of C-14 Data – Discussion, Radiocarbon, 19, 355–363, 1977.

Suarez, A. E. and Ondov, J. M.: Ambient aerosol concentrations of elements resolved by size and by source: Contributions of some cytokine-active metals from coal- and oil-fired power plants, Energy Fuels, 16, 562–568, 2002.

Subramanian, R., Donahue, N. M., Bernardo-Bricker, A., Rogge, W. F., and Robinson, A. L.: Insights into the primary-secondary and regional-local contributions to organic aerosol and PM$_{2.5}$ mass in Pittsburgh, Pennsylvania, Atmos. Environ., 41, 7414–7433, 2007.

Szidat, S., Jenk, T. M., Gaggeler, H. W., Synal, H. A., Fisseha, R., Baltensperger, U., Kalberer, M., Samburova, V., Wacker, L., Saurer, M., Schwikowski, M., and Hajdas, I.: Source apportionment of aerosols by C-14 measurements in different carbonaceous particle fractions, Radiocarbon, 46, 475–484, 2004.

Tanner, R. L., Parkhurst, W. J., and McNichol, A. P.: Fossil sources of ambient aerosol carbon based on C-14 measurements, Aerosol Sci. Technol., 38, 133–139, 2004.

Taylor, S. R. and McLennan, S. M.: The Continental Crust: Its Composition and Evolution. , edited by: Publications, B. S., Oxford, Boston, Palo Alto, Victoria, 1985.

Thorpe, A. and Harrison, R. M.: Sources and properties of non-exhaust particulate matter from road traffic: A review, Sci. Total Environ., 400, 270–282, 2008.

Tsai, J.-H., Lin, K.-H., Chen, C.-Y., Ding, J.-Y., Choa, C.-G., and Chiang, H.-L.: Chemical constituents in particulate emissions from an integrated iron and steel facility, J. Hazard. Mater., 147, 111–119, 2007.

Viana, M., Kuhlbusch, T. A. J., Querol, X., Alastuey, A., Harrison, R. M., Hopke, P. K., Winiwarter, W., Vallius, A., Szidat, S., Prevot, A. S. H., Hueglin, C., Bloemen, H., Wahlin, P., Vecchi, R., Miranda, A. I., Kasper-Giebl, A., Maenhaut, W., and Hitzenberger, R.: Source apportionment of particulate matter in Europe: A review of methods and results, J. Aerosol Sci., 39, 827–849, 2008.

Virkkula, A., Teinilä, K., Hillamo, R., Kerminen, V.-M., Saarikoski, S., Aurela, M., Viidanoja, J., Paatero, J., Koponen, I. K., and Kulmala, M.: Chemical composition of boundary layer aerosol over the Atlantic Ocean and at an Antarctic site, Atmos. Chem. Phys., 6, 3407–3421, doi:10.5194/acp-6-3407-2006, 2006.

Wang, W., Wu, M. H., Li, L., Zhang, T., Liu, X. D., Feng, J. L., Li, H. J., Wang, Y. J., Sheng, G. Y., Claeys, M., and Fu, J. M.: Polar organic tracers in PM$_{2.5}$ aerosols from forests in eastern China, Atmos. Chem. Phys., 8, 7507–7518, doi:10.5194/acp-8-7507-2008, 2008.

Watson, J. G., Robinson, N. F., Fujita, E. M., Chow, J. C., Pace, T. G., Lewis, C., and Coulter, T.: CMB8 Applications and Validation Protocol for PM$_{2.5}$ and VOCs, US EPA, USA, 1998.

Weitkamp, E. A., Lipsky, E. M., Pancras, P. J., Ondov, J. M., Polidori, A., Turpin, B. J., and Robinson, A. L.: Fine particle emission profile for a large coke production facility based on highly time-resolved fence line measurements, Atmos. Environ., 39, 6719–6733, 2005.

Weitkamp, E. A., Lambe, A. T., Donahue, N. M., and Robinson, A. L.: Laboratory Measurements of the Heterogeneous Oxidation of Condensed-Phase Organic Molecular Makers for Motor Vehicle Exhaust, Environ. Sci. Technol., 42, 7950–7956, 2008.

Yttri, K. E., Dye, C., and Kiss, G.: Ambient aerosol concentrations of sugars and sugar-alcohols at four different sites in Norway, Atmos. Chem. Phys., 7, 4267–4279, doi:10.5194/acp-7-4267-2007, 2007.

Zhang, Y. X., Schauer, J. J., Zhang, Y. H., Zeng, L. M., Wei, Y. J., Liu, Y., and Shao, M.: Characteristics of particulate carbon emissions from real-world Chinese coal combustion, Environ. Sci. Technol., 42, 5068–5073, 2008.

Zheng, M., Ke, L., Edgerton, E. S., Schauer, J. J., Dong, M. Y., and Russell, A. G.: Spatial distribution of carbonaceous aerosol in the southeastern United States using molecular markers and carbon isotope data, J. Geophys. Res.-Atmos., 111, D10S06, doi:10.1029/2005JD006777, 2006.